Cellular Communications Coverage Prediction Techniques: A Survey and Comparison

OLAONIPEKUN OLUWAFEMI ERUNKULU, (Member, IEEE),
ADAMU MURTALA ZUNGERU, (Senior Member, IEEE),
CASPAR K. LEBEKWE, (Member, IEEE), AND
JOSEPH M. CHUMA, (Member, IEEE)
Department of Electrical, Computer and Telecommunications Engineering, Botswana International University of Science and Technology, Palapye, Botswana

Corresponding author: Adamu Murtala Zungeru (zungerum@biust.ac.bw)

ABSTRACT A lot of effort and time is utilized in the planning and building of the cellular wireless networks to use minimum infrastructural components to provide the best network coverage as well as delivery of quality of service. Generally, path loss models are used for the prediction of wireless network coverage. Therefore, detailed knowledge of the appropriate path loss model suitable for the proposed geographical area is needed to determine the coverage quality of any wireless network design. However, to the best of our knowledge, despite the importance of path loss models, as used for the prediction of wireless network coverage, there doesn't exist any comprehensive survey in this field. Therefore, the purpose of this paper is to survey the existing techniques and mechanisms which can be addressed in this domain. Briefly, the contributions of this paper are: (1) providing a comprehensive and up to date survey of the various network coverage prediction techniques, indicating the different frequency ranges the models were developed, (2) the different suitable terrains for each of the model and the best suit mobile generation were presented, and lastly, (3) providing comparative analysis to aid the planning and implementation of the cellular networks.

INDEX TERMS Path loss model, prediction, wireless, propagation scenarios, mobile generations, signal.

I. INTRODUCTION

The remarkable changes experienced by the development of mobile communication system over the last few years has led to severe challenges to the planning of mobile wireless networks. This fruition journey of the first-Generation (1G) network started back in the year 1979 and has progressed to the presently explored Fifth Generation (5G) network. Each new generation is usually built upon the present generation's needs, which led to research and development for a better technology that will accommodate the needs, capacities, proper availability to the end-user. With this exponential increase in the use of mobile-connected devices as well as the constant expansion of mobile communication networks, the effective provision of the coverage of the mobile networks is imperative for the delivery of quality of service (QoS) [1]. Radio propagation can be defined as the behaviour of radio

waves experienced while signals are transmitted from one point to another [2]. Such phenomena like absorptions, reflections, scattering, refractions, among others, affect the radio wave [3]. Therefore, mobile network coverage prediction is a vital and essential task in the planning and deployment of cellular technology.

Unlike the other communication systems, the most complex among them is the wireless communication system, due to channel fading characteristics, which are decided based on the environment where radio propagation occurs. Furthermore, each terrain or environment has a defining characteristic of propagation [4]. Therefore, the determination of the specific propagation model to predict the coverage area in a different environment is important.

Before the mass deployment of cellular networks, detailed knowledge of the wireless channel model, as well as the propagation models, are essential. The channel model illustrates the characteristic of how the transmitted signal can be affected based on medium and environmental conditions.

The associate editor coordinating the review of this manuscript and approving it for publication was Barbara Masini.

The effects of the propagated signals are usually mathematically represented. In other words, the channel model addresses the medium in which the signal is transmitted. On the other hand, propagation models predict the distance the signal will travel before attenuation, which is the coverage area of the transmitted signal. The propagation models require the properties of the proposed geographical area to determine the coverage quality of any wireless network design.

Various researches on channel prediction techniques had been carried out [5]–[9] for various wireless channel systems such as multiple input and multiple output systems (MIMO) [10]–[13]. Reference [14] surveyed wireless channel standardized models and radio propagation models for MIMO systems while [15] presented the preliminary outcomes of extensive research on mmWave massive MIMO. Some of the models discussed are not only used for cellular communication but other wireless systems such as unmanned aerial vehicle (UAV) [16], [17], digital terrestrial television (DTT) system [18], Digital Video Broadcasting - Terrestrial DVB-T [19], [20].

Conventionally, the cellular coverage map is built by service providers using a time consuming and an expensive campaign known as a drive-test. The Radio Frequency (RF) parameters are subject to various tuning process to determine the optimum values. According to various researches, the prediction of network coverage areas theoretically, is quite difficult to actualize [21]–[24]. However, wireless network coverage prediction can be solved mathematically by using computer algorithms (software simulations) and initial assumptions for the planning of any wireless communication networks, and it mathematically estimates the anticipated network characteristics which assist in the design process. The models are expected to be as precise as possible for the easier development of wireless networks [25].

On the other hand, the frequency bands have been exploited worldwide for various mobile wireless communication infrastructures. As a result of this, organizations were set up to govern the worldwide allocation of spectrum for the 5G networks systems. These organizations to provide the guidelines are the International Telecommunication Union for Radiocommunication sector (ITU-R) [26] and the World Radio Conference (WRC-15) [27]. Presently, all wireless systems make use of spectrum in the range 300MHz to 3GHz band while the future communication network (5G and so on) will use the millimeter wave (mmWave) band as the channel. These frequency bands are known to have different channel propagation characteristic that affects signal transmission. Therefore, the accurate selection of the propagation model for different frequency bands and terrains is essential.

In this paper, a comprehensive comparative and up to date study of the various network coverage prediction techniques at different frequency ranges, the best suit mobile generation, as well as the suitable terrains for each of the models was carried out. It had also provided a comparative analysis to aid the planning and implementation of the cellular networks.

The paper focuses on the propagation models for large-scale fading in mobile communication.

The rest of this paper is organized as follows: Section II highlights related work. Section III discusses the propagation phenomena of wireless propagation. In Section IV, the various propagation models used for coverage prediction for cellular communications are discussed. In Section V, the classification of the models is presented. Section VI discussed the emerging technology, and finally, conclusions are drawn in Section VII.

II. RELATED WORK
Over the years, many studies have investigated and surveyed the propagation models for various frequency bands in different environments (indoor and outdoor) and scenarios (line of sight and non-line of sight). Most of the surveys done had focused mainly on a few PL models. Prior research had focused on models applicable to one or two of the cellular communication networks. Table 1 presents a comparison of a few surveyed and reviewed research work on PL models.

III. PROPAGATION PHENOMENA
The mechanism for wireless propagation is quite complicated and diverse. Signals are not bonded to any physical conductor or cable like the case of wired transmission; instead, it makes use of EM wave, which is an unguided and unbounded system for the transmission of signals through the medium. Due to the attenuation of the transmitted signals, such phenomena like diffraction, reflections, scattering, refractions, among others, affect the radio wave [28], as illustrated in Figure 1.
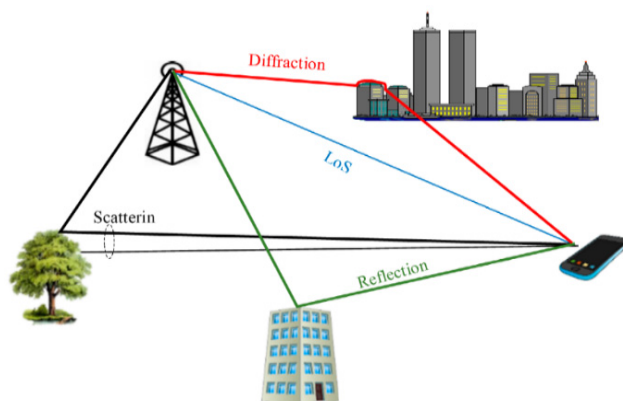

FIGURE 1. Illustration of the propagation phenomena.

Diffraction occurs in a scenario where the transmitted signal encounters an obstructing structure whose size is larger than the wavelength of the transmitted signal [29]. It allows signals to be transmitted around the surface of the earth's curve. The signals are usually diffracted at a sharp edge of the large structure where the waves are scattered. Diffraction occurs in Non-Line of Sight (NLoS) scenarios, irrespective of the environment (Rural or Urban) [28], making it possible to provide effective mobile coverage in urban areas.

TABLE 1. Comparison of related work on path loss models.

Title	Citations	Year	Description	Pros	Cons	The uniqueness of this paper
A Comprehensive Survey of Electromagnetic Propagation Models	[31]	2017	Surveyed and compared different Propagation models such as Okumura's Model, Hata Model, Longley rice Model among others	Illustrated various applicable terrains and respective equations for the different models	The models surveyed were not comprehensive, not all the applicable frequency range of the models were illustrated	This paper addresses more PL models and provided all the information regarding the models' equations as well as the applicable terrains.
A Survey of Wireless Path Loss Prediction and Coverage Mapping Methods	[32]	2013	The paper surveyed comprehensive coverage predictive models as well as identifying the differences of the models.	The survey covered more PL models, categorized the models	Fewer models' equations were provided, detailed terrain information and frequency ranges were not provided	This survey included the PL models developed for mmWave making it to be an up-to-date survey. Every frequency range and equations of the models were provided
A Survey of Various Propagation Models for Mobile Communication	[33]	2003	The paper reviewed information on the various PL models for both indoor and outdoor environments. Classified the models. The characteristics of the radio channel were also discussed	The survey provided all the needed equations of the PL models, the accuracy and complexity of the models were discussed	PL models developed after the year 2003 were not covered. No graphical expression of the models' performance.	This survey accommodated other PL models developed to date. Graphical expression of the models' performances was included
Radio Wave Propagation Mechanisms and Empirical Models for Fixed Wireless Access Systems	[34]	2010	The paper surveyed the basic mechanisms that influence the propagation of electromagnetic waves. Empirical models were surveyed	Comparison of the PL models accuracy for LOS/NLOS location division and terrain type were done, graphical expressions of the PL model were plotted.	The surveyed models were very few and focused only on WiMAX networks. The frequency ranges of all the models were not specified.	This survey covered an in-depth survey of the models for the 1G to 5G networks.
Millimeter-Wave Distance-Dependent Large-Scale Propagation Measurements and Path Loss Models for outdoor and Indoor 5G Systems	[35]	2016	The paper presented mmWave propagation measurements for both outdoor and indoor scenarios. It also investigated five PL models.	The PL models were explained in detail, In-depth knowledge, comparison and plotting of the PL models were implemented	The focus was on models for 5G networks alone	This paper covered all the other networks PL models, indicating other models that could be used for predicting coverage area

Scattering is the redirection of a transmitted signal away from its initial propagation direction, usually due to encountering of objects with smaller or comparable wavelength to that of the transmitted signal, causing the signal to spread out (scatter) into a various number of directions. Scattered waves in mobile communication systems could be formed by rough or bumpy surfaces as well as small objects, such as foliage, street signs, lamp posts, and building stairs. Among the phenomena mentioned, the prediction of scattering is the most difficult [30]. Therefore, comprehensive knowledge of various object physical details is useful in the accurate prediction of scattered signals.

Reflection occurs when a signal impinges a solid surface with dimensions that are much wider than the transmitted signal wavelength resulting in the reflection of the transmitted signal in another direction [31]. When a wave is reflected, it could either cause an increase or decrease of the overall strength of the received signal depending on the phase sum of the NLoS and LoS components of the transmitted signal at the endpoint. Furthermore, the received signal level tends to be unstable, where lots of waves are reflected. This phenomenon is usually referred to as multipath fading [28].

Generally, the atmospheric refractive index is always changing, resulting in the refraction of radio waves. The knowledge of radio wave refraction is essential in the designing of the wireless system since the EM waves do propagate along a curved line and not a straight line. This makes the coverage area of a base station to be habitually larger. However, the signal strength of the received signal fluctuates, too, due to the variations of the atmospheric parameters. Multipath fading also causes fluctuation of the received signal around its mean value at certain locations. Therefore, modelling of the signal received is a combination of small-scale fading as well as the large-scale fading effects.

IV. PROPAGATION MODELS

Signals transmitted over the RF channel of mobile communications are subject to losses due to fading, scattering, penetration losses, among others. These problems can be easily reduced if the propagation characteristic of the channel can be predicted using propagation models. These are set of mathematical expressions, algorithms as well as diagrams used for representing the characteristics of an RF of a given scenario and environment. These mathematical equations are used for estimating the transmitter signal strength in a particular terrain. The models are usually designed for distinct scenarios due to factors such as the operating frequency, the distance between the transmitter and receiver, weather conditions, among others [25]. Overestimation or underestimation of path loss (PL) occurs when the wrong model is chosen for a scenario as well as the wrong prediction of interference between the cells [36]. An understanding of PL in a given geographical area provides better network planning. PL is the decrease of an electromagnetic wave power density as it spreads or travels through a medium, and it is illustrated by (1)

$$PL\,(dB) = 10\log\left(\frac{P_t}{P_r}\right) \tag{1}$$

where P_t is the transmitted power and P_r is the received power.

PL is subject to many parameters such as transmitter power, the transmitter, the receiver antenna type and its gain, the receiver power, the structure of the channel, the effect of the refraction, reflection, and diffraction. The purpose of PL modelling is to estimate the extent of the radio signal attenuation over a distance, which is essential for designing the wireless network systems [37].

In mobile communications, transmitted signals arrive at a receiver unit via multiple paths. The signal along each path experiences different path delay with respect to the line of sight (LoS) because each path distance taken between the receiver and transmitters is larger than the LoS path distance. The signal along the multipath experience attenuation due to the terrain makeup of those paths and arrive at the receiver at different angles of arrival (AOA) [38]–[40]. The estimate of the delay and joint angle for these multipath signals is determined by adaptive processing methodology [33]. Stochastic processes are usually applied by fading models in describing the distribution of the signal received, and these models are beneficial for the simulation of the propagation channels to predict the coverage area as well as the system performance. The models are generally derived from the data acquired as a result of lots of measurement campaign carried out and are usually designed for frequency ranges [41].

In the deployment of mobile communication, three different types of environments are majorly considered, namely: Rural, Suburban, and Urban. These give insight into the various environment or areas where wireless communications are deployed. The Rural Area usually do not have big obstacles such as tall buildings or trees in the path of the propagated signals, influence of terrain height. Suburban areas are villages that are populated with buildings and trees. Still, an average height, interferences are mild, while the Urban Area are big cities with the enormous structure of building with several floors or bigger village that has scattered thick and tall trees.

Generally, propagation models can be classified based on the principle approach used in the development of the models, which are empirical models and deterministic models. Table 2 highlights some of the notations and parameters used in this paper.

TABLE 2. Summary of notation and parameters.

Notation	Definitions
d	distance between transmitter and receiver along line of sight path in km
h_{re}	height of receiver above ground in m
h_{te}	height of transmitter above ground in m
P_t	transmitter (Base station) power
P_r	receiver (mobile station) power
f_c	frequency carrier in MHz or GHz
G_{te}	transmitter's antenna gain
G_{re}	receiver's antenna gain
λ	wavelength in m
C	speed of light in m/s
w	is the width of the street in meters
h_{roof}	building roof height
h_B	the average building height
d_o	reference distance
d_B	breakpoint distance

Empirical Models (Statistical Model): Empirical models are developed from observations and measurements. These models are based on extensive experimental data and statistical analysis, which enable us to compute the received signal level in a given propagation medium. An empirical model considers all environmental impacts or effects on the development of the model. Unfortunately, the model is more accurate and effective when it is deployed in environments that are similar to the environment where it was developed [42]. For this reason, the models are more accurate and suitable at the area where the measurement campaigned was carried out and needs adaption for different areas. Some of the known and widely used empirical models for the prediction of network coverage area are discussed. The PL models are given in dB except otherwise stated.

A. FREE SPACE LOSS

The FSPL model is the simplest PL model [43], used for predicting an RF signal strength at a specific distance in free space. Equation (2) shows the relationship between the power of the transmitter and the receiver, where (3) illustrates the FSPL in dB

$$P_r = P_t G_{te} G_{re}\left(\frac{\lambda}{4\pi d}\right)^2 \tag{2}$$

$$FSPL = 20\left(\log(d) + \log(f) + \left(\frac{4\pi}{C}\right)\right) - G_{te} - G_{re} \tag{3}$$

where P_r is received power, P_t is transmitted power, G_{te} is transmitter antenna gain, G_{re} is receiver gain, λ is the wavelength, d is the transmitter, and the receiver distance, f is the carrier frequency, and C is the speed of light.

Free space means a clear and unobstructed line-of-sight transmitter to receiver (T-R) terrain. The free space propagation model predicts that the received power P_r decays as a function of the distance d between the transmitter and the receiver. In reality, reflection, diffraction from objects, and other losses occur and must be considered while approximating the signal strength at any location.

B. OKUMURA ET AL. MODEL

This is the simplest model used for estimating PL, and it gives excellent accuracy in the PL estimation in wireless communication systems. It is a widely used model for network coverage prediction in urban areas but limited by tall blocking structures. A study was carried out by Okumura [44] to determine the reduction in power density over distance in the city of Tokyo, Japan. The data collected were used in developing the model. The basic prediction formula is shown by (4):

$$PL_{Mean} = FSPL + A(f, d) - G(h_{te}) - G(h_{re}) - G_{Area} \quad (4)$$

where PL_{Mean} is the PL median value, $FSPL$ is the free space propagation loss, $A(f, d)$, is the median attenuation as a function of the selected frequency f, and the corresponding distance between the base station (BS) and the mobile station (MS). $G(h_{te})$ and $G(h_{re})$, are the Gain factors in dB for the antenna of BS (transmitter) and that of MS (receiver respectively. h_{te} and h_{re} are the effective heights of the base station and the mobile unit, respectively. G_{Area}, is the gain due to the type of terrain the system is operating. The value of $A(f, d)$ and G_{Area} can be obtained from the empirical curves while $G(h_{te})$ and $G(h_{re})$ values are calculated from formulas, as shown in the Eqns. (5a-5c).

$$G(h_{te}) = 20log\frac{h_{te}}{200}, \ 100 \le h_{te}, \quad 30mG(h_{te}) \quad (5a)$$

$$G(h_{re}) = 10log\frac{h_{re}}{3}, \quad h_{re} \le 3m \quad (5b)$$

$$G(h_{re}) = 20log\frac{h_{re}}{3}, \quad 10m > h_{re} > 3m \quad (5c)$$

This model was designed for the frequency range of 150MHz to 1.92GHz (typically extended up to 3 GHz) with cell diameters of 1 to 100 km, the BS Antenna height ranging from 30m - 1 km and 1-10 m antenna height for MS. It is very practical and has become a standard for system planning in Japan. The major disadvantage of this model is its slow response to rapid changes in terrain profile.

Information on the terrain, such as average slope and terrain modulation height, can be qualitatively incorporated in the model [45].

C. OKUMURA-HATA MODEL

Hata is an extension of the Okumura model [46], and the model formula was derived from the Okumura's curves to make it applicable to different terrains apart from Tokyo [25]. A lot of propagation models are extensions of the Okumura-Hata model. The model is suited in the configuration for large cells, where the BS is higher than any surrounding obstacles. Scattering, refraction, and diffraction is the main propagation loss for this model [36]. The model has its limitations based on frequency, range as well as the BS height since it is a macrocell model. The model is designed for the frequency range of 150 MHz to 1.5Ghz, which is shorter than that of the Okumura model. The BS and MS effective heights are in the range of 30-200m and 1-10m, respectively, and for a distance of 1 km-20 km.

Okumura-Hata models have two forms. The PL of the first form is illustrated by (6):

$$PL = FSPL + A_{exc} - H_{cb} - H_{cm} \quad (6)$$

where FSPL is already known, A_{exc} is the excess PL (as a function of distance and frequency) while H_{cb} and H_{cm} are the correction factors for BS and MS, respectively. The second form is the most common form used, which was derived from the curve fitting of Okumura's original results. The model is expressed by (7)

$$PL_{Urban} = 69.55 + 26.16log(f_c) - 13.82\log(h_{te}) - a(h_{re})$$
$$+ (44.9 - 6.55logh_{te})\log(d) + C_m \quad (7)$$

where frequency f_c is given in MHz, d is the distance between BS and MS in km, h_{te} and h_{re} are the effective heights of both the BS and MS, respectively. C_m is dependent on the environment. The correction factor for the MS antenna height is the $a(h_{re})$, usually a function of the coverage area size.

The model assumes no presence of dominant obstacles between the BS and the MS, and that the terrain profile changes only slowly [47], unfortunately, these assumptions are not binding in many other terrains, hence, the correction of the model to estimate the propagation loss accurately [48]. Therefore, the mobile correction factors $a(h_{re})$ of the MS antenna height for the different area are represented by (8) through (13) as:

Small-to-medium-sized cities;

$$a(h_{re}) = (1.1log(f_c) - 0.7)h_{re} - (1.56log(f_c) - 0.8) \ C_m = 0 \quad (8)$$

Large cities;

$$a(h_{re}) = \begin{cases} 8.29(log1.54h_{re})^2 - 1.1, & for \ f \le 300MHz \\ 3.2(log11.75h_{re})^2 - 4.97, & for \ f \ge 300MHz \end{cases}$$
$$C_m = 0 \quad (9)$$

Suburban area:

$$C_m = -2\left[log(f_c/28)\right]^2 - 5.4 \quad (10)$$

Therefore, the PL for the suburban environment is stated in (11)

$$PL_{Suburban} = PL_{Urban} - 2\left[log\left(f_c/28\right)\right]^2 - 5.4 \quad (11)$$

For rural area

$$C_m = -4.78\left[log\left(f_c\right)\right]^2 + 18.33log\left(f_c\right) - 40.98 \quad (12)$$

Therefore, the PL for the rural environment is stated in (13)

$$PL_{rural} = PL_{urban} - 4.78\left[log\left(f_c\right)\right]^2 + 18.33log\left(f_c\right) - 40.98 \tag{13}$$

Additionally, the $a\left(h_{re}\right)$ function in the rural and suburban environments is the same as the small-to-medium-sized cities.

D. COST CHANNEL MODELS

The Cooperation in Science and Technology (COST) is a European funded program. COST 207 [49] was the first channel model derived for the standardization of GSM. Unfortunately, the PL model for different propagation scenarios was not considered. Rather, a different environment of four power-delay profile was accounted for [50]. The COST 231 [51] models focused on the PL models resulting in COST Hata models and COST Walfish-Ikegami. The COST 231 described further in the sub-section A as:

1) COST 231-HATA MODEL

The frequency range limitation of the Okumura-Hata model was solved in the COST 231-Hata model [51]. The model is the advancement of the Hata model, which was developed to accommodate more elaborated frequency ranges up to 2 GHz, frequency which is used for 2G and 3G Cellular network [52]. Experimental measurements were carried out in several cities in Europe by the European Union Forum for cooperative scientific research to develop the model [46]. The model is useful in predicting the coverage area in urban environments at a frequency range of 1.5 GHz to 2 GHz. One of its key advantages is the availability of correction factors for rural (flat), urban, as well as the suburban environments [52], [53]. The PL is computed using (14) as:

$$PL_{COST} = 46.3 + 33.9log(f_c) - 13.82\log\left(h_{te}\right) - a\left(h_{re}\right)$$
$$+ \left(44.9 - 6.55\log\left(h_{te}\right)\right)log(d) + C_m \quad (14)$$

where the correction factor

$$C_m = \begin{cases} 0dB, & suburban\ environments \\ 3dB, & for\ urban\ environment \end{cases}$$

For suburban and rural areas

$$a\left(h_{re}\right) = \left(1.1log(f_c) - 0.7\right)h_{re} - \left(1.56log(f_c) - 0.8\right) \tag{15}$$

For urban areas

$$a\left(h_{re}\right) = 3.2\left(log11.75h_{re}\right)^2 - 4.97,\ \&\ for\ f > 400MHz \tag{16}$$

2) COST-231-WALFISCH-LKEGAMI MODEL

This model was developed by the combination of J. Walfisch and F. Ikegami models. The model was then enhanced by the COST 231 project [54]–[56]. The model employs the theoretical Walfisch-Bertoni model [57] to acquire multiple diffraction loss for BS antenna heights but uses measured data for low BS antenna heights. The model gives accurate path loss estimation by considering both LoS and Non-Line of sight (NLoS) scenarios, building height causing obstruction, the street width, and other urban environment factors [58]. This makes it very suitable for suburban and rural area path loss prediction [59]. It is developed for urban areas and it takes into consideration obstructing building height and street width as well as other factors related to the urban environment. This model is developed to distinguishes between the NLoS and LoS scenarios.

For the LoS, the total path loss is given by (17):

$$PL_{LOS} = 42.6 + 26\log d + 20\log f \tag{17}$$

For the NLoS, the model consists of three basic components which are L_0 for free-space loss, L_{rts} for diffraction and scattering losses from rooftop to street and L_{ms} for the multiscreen diffraction loss, the total path loss is given by (18)

$$PL_{NLOS} = \begin{cases} L_0 + L_{rts} + L_{ms}, & L_{rts} + L_{ms} > 0 \\ L_0, & L_{rts} + L_{ms} \leq 0 \end{cases} \tag{18}$$

where each component is defined as

$$L_0 = 32.4 + 2\log d + 20\log f \tag{19a}$$

$$L_{rts} = -16.9 - 10logW + 10logf + 20log\Delta h_m + L_{ori} \tag{19b}$$

$$L_{ms} = L_{bsh} + k_a + k_d\log d + k_f\log f + 9\log B \tag{19c}$$

where B is the distance between the buildings. L_{bsh} is the shadowing gain, which occurs when the building rooftops are lower than the BS antenna height and factor k_a signify the increase of PL as a result of reduced BS antenna height.

Consider this abbreviation; $\Delta h_{te} = h_{te} - h_{roof}$. L_{bsh} and k_a are given by (20a) and (20b) respectively, which is given by:

$$L_{bsh} = \begin{cases} -18\log\left(1 + \Delta h_{te}\right), & h_{te} > h_{roof} \\ 0, & h_{te} \leq h_{roof} \end{cases} \tag{20a}$$

$$K_a = \begin{cases} 54, & h_{base} < h_{roof} \\ 54 - 0.8\Delta h_{te}, & d \geq 0.5km\ \&\ h_{roof} \leq h_{te} \\ 54 - 0.8\Delta h_{te}\dfrac{d}{0.5}, & d < 0.5km\ \&\ h_{roof} < h_{te} \end{cases} \tag{20b}$$

The dependency of the losses due to multiscreen diffraction are described by the terms k_d and k_f as a function of distance and frequency of operation, respectively. The terms k_d and k_f

are illustrated by (20c), and (20d) respectively:

$$k_d = \begin{cases} 18 - 15 \left(\dfrac{\Delta h_{te}}{h_{roof}} \right), & h_{te} \leq h_{roof} \\ 18, & h_{te} > h_{roof} \end{cases} \quad (20c)$$

$$k_f = -4 \begin{cases} 0.7 \left(\dfrac{f}{925} - 1 \right) \text{medium-sized and suburban} \\ 1.5 \left(\dfrac{f}{925} - 1 \right) \text{metropolitan center} \end{cases}$$

(20d)

while

$$L_{ori} = \begin{cases} -10 + 0.354\emptyset, & 0° \leq \emptyset < 35° \\ 2.5 + 0.075 \left(\emptyset - 35 \right), & 35° \leq \emptyset < 55° \\ 4.0 - 0.114 \left(\emptyset - 55 \right), & 55° \leq \emptyset \leq 90° \end{cases} \quad (20e)$$

From (19b), W is the width of the street in meters and $\Delta h_{re} = h_{roof} - h_{re}$ while L_{ori} is illustrated in (20e)

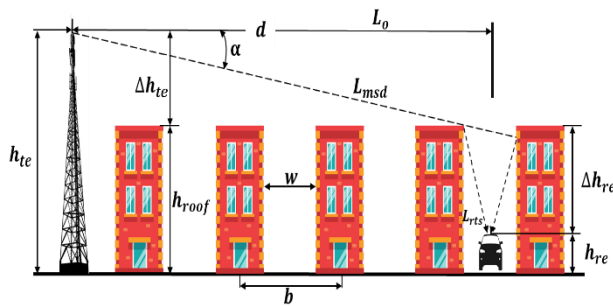The parameters' definition is illustrated in Figure 2.

FIGURE 2. Model parameters definition.

COST-231-Walfisch-Ikegami model was developed to predict PL for the frequency range 800 MHz - 2 GHz, the BS antenna height range from 4 - 50m for a distance of 0.02 - 5 km. The height of the MS antenna is usually not more than 3m [56].

The main drawback of the COST-231-Walfisch-Ikegami model is that it does not take the multiple reflections from buildings into consideration but focuses on the effects of the roof to street diffraction [55]. Much research had gone into improving the model to accommodate the multiple diffraction loss from buildings by using the deterministic image method of ray tracing [59]. The estimation of multiple-diffraction loss, as well as the final diffraction loss term performance based on the Uniform Theory of Diffraction, was given in [60], [61].

3) COST 259

This is a directional channel model (DCM), developed within the initiative of the European research [62]. The research was based on modelling the directional properties of the channel, which gave further research studies to the diversity and adaptive antenna systems. The model accommodated not only the PL but most of the aspects of the wireless channel

such as fast fading, polarization as well as the delay and angular spread [63]. Measurement in the frequency range of 0.45 - 5 GHz and bandwidths up to 10 MHz were used to derive the model. This model is developed to distinguishes between the NLoS and LoS scenarios.

For the LoS, the PL is given by (21):

$$PL(d) = max \left(\frac{h_{te} - h_B}{h_{te}} \frac{d_{CO} - d}{d_{CO}}, 0 \right) \quad (21)$$

where d_{CO} is a cut-off distance. All other parameters remain as described.

For the NLoS, the PL is given by (17):

COST 231-Hata Model or COST-231-Walfisch-Bertoni [57] can be used for the prediction of PL under the NLoS conditions by applying some extensions [51], [64].

E. ECC-33 MODEL

The model was developed by the Electronic Communication Committee (ECC) by extrapolating the original measurement data from Okumura research [65], [66]. The Okumura model and COST-231 model were both limited to the maximum frequency of 1.5 GHz and 2 GHz, respectively. Still, with the extrapolation method, the ECC-33 model was modified to predict PL for frequency greater than 3 GHz [67]. It was adapted for both medium and large cities and also can be used for suburban and open areas due to the inclusion of correction factors [68]. The model is more effective for the frequency range of 700 MHz to 3.5 GHz [68]. In this model, the path loss is given by (22)

$$PL_{ECC}(dB) = A_{fs} + A_{bm} - G_{te} - G_{re} \quad (22)$$

where A_{fs} is the free space attenuation, A_{bm} is PL due to basic median, G_{te} is the BS antenna gain factor and G_{re} is the MS antenna gain factor. (23a) – (23c), individually define them.

$$A_{fs} = 92.4 + 20 \log_{10}(d) + 20 \log_{10} f \quad (23a)$$

$$A_{bm} = 20.41 + 9.83 \log_{10}(d)$$
$$+ 7.894 \log_{10} f + 9.56 [\log_{10} f]^2 \quad (23b)$$

$$G_{te} = \log \left(\frac{h_{te}}{200} \right) [13.98 + 5.8(\log(d))^2] \quad (23c)$$

where for medium cities is used (23d)

$$G_{re} = [42.57 + 13.7 \log(f)][\log(h_{re}) - 0.585] \quad (23d)$$

And, for large cities is used (23e)

$$G_{re} = 0.0759 h_{re} - 1.862 \quad (23e)$$

F. ERICSSON 9999 MODEL

The Ericsson 9999 model [69] was developed by Ericsson [70] as an extension or improvement of the Okumura-Hata and Cost 231-Hata Models [69]. The parameters of the model can be adjusted per given scenario [25]. It was developed to accommodate frequency up to 2 GHz, but the model could be adapted for higher frequencies and different application scenarios due to the inclusion of tuning

parameters in the model [36], [69]. In this model, the path loss is given by (24) as:

$$PL = a_0 + a_1 \log_{10}(d) + a_2 \log_{10}(h_{te})$$
$$+ a_3 \log_{10}(h_{te}) \log_{10}(d) - 0.2 \left(\log_{10} 11.75 h_{re} \right]^2 \right)$$
$$+ g(f) \qquad (24)$$

where $g(f)$ is given by (24a)

$$g(f) = 44.49 \log_{10}(f) - 4.78 \left(\log_{10}(f) \right)^2 \qquad (24a)$$

and a_0, a_1, a_2 *and* a_3 values are given in Table 3

TABLE 3. Ericsson model parameters [71].

Environment	Urban	Suburban	Rural
a_0	36.2	43.20*	45.95*
a_1	30.2	68.93*	100.6*
a_2	12.0	12.0	12.0
a_3	0.1	0.1	0.1

G. STANFORD UNIVERSITY INTERIM (SUI) MODEL

Stanford University, along with the 802.16 IEEE group [72], conducted extensive research to develop a propagation model suitable for the Worldwide Interoperability for Microwave Access (WiMAX) applications for suburban environments [66]. The study led to the development of the SUI propagation loss model, and the research was an advanced work and analysis of the AT&T wireless research and that of Erceg *et al.* [73]. The model is applicable for frequencies above 1900 MHz [74]. In order to find the median PL, the terrains are categorised into three groups A, B, C: Terrain A denotes a terrain with extreme PL due to hilly terrains and also very densely populated. Terrain B represents an environment with moderate PL, such as a suburban environment with rare vegetation (hilly environment) or high vegetation (flat terrain), while terrain C has the least PL condition, usually flat area with light tree densities.

The general scenarios for the stated categories are as follows: Cells are lesser than 10 km in radius, the MS antenna height is in the range of 2 m to 10 m, BS antenna height range from 15 m to 40m with a high network coverage requirement of 80% to 90%. The research lead to the development of three types of the model, which are Basic SUI Model, SUI Model with correction factors and Extended SUI Model.

1) BASIC SUI MODEL

This model was based on Erceg's model [72], and it was IEEE proposed to estimate PL for frequencies around 2 GHz and with MS antenna height below 2 m. the model is quite suitable for suburban environments [75].

The following (25) defines the PL median as:

$$PL_B(dB) = A + 10\gamma \log \left(\frac{d}{d_0} \right) + s \qquad (25)$$

where *s* is the shadowing effect dependent on the terrain with value *8.2 dB < s< 10.6*, *d* is the distance between BS and MS antennas in m, d_0 is 100 m (i.e. $d > d_0$). A is given by (26a)

$$A = 20\log \left(\frac{4\pi d_0}{\lambda} \right) \qquad (26a)$$

where λ is the wavelength, γ is path loss exponent (PLE) given by (26b):

$$\gamma = a - bh_{te} + \frac{c}{h_{te}} \qquad (26b)$$

where a, b and c are constants that depend on the terrain category are given in Table 4.

TABLE 4. SUI model parameters [76].

Model	Terrain A	Terrain B	Terrain C
A	4.6	4.0	3.6
B	0.0075	0.0065	0.005
C	12.6	17.1	20

2) SUI MODEL WITH CORRECTION FACTORS

This version is the most used in PL estimation. Correction factors were introduced to cater for frequencies above 2 GHz and MS antenna heights, h_{re}, ranging between 2 and 10 m, as illustrated by (27)

$$PL_b(dB) = A + 10\gamma \log \left(\frac{d}{d_0} \right) + s + \Delta L_{bf} + \Delta L_{bh} \qquad (27)$$

where ΔL_{bf} is the correction factor for the frequency and ΔL_{bh}, is the height correction factors defined by (28a) and (28b), respectively.

$$\Delta L_{bf} = 6.0\log \left(\frac{f}{2000} \right) \qquad (28a)$$

$$\Delta L_{bh} = \begin{cases} -10.8\log \left(\frac{h_{re}}{2} \right) & \text{terra in type A and B} \\ -20\log \left(\frac{h_{re}}{2} \right) & \text{for terra in type C} \end{cases} \qquad (28b)$$

3) EXTENDED SUI MODEL

This extended SUI model [77] was IEEE 802.16 proposed to modify the MS height correction factor ΔL_{bh} in (42). A new procedure for calculating the reference distance d_0 was introduced by this modification, thereby, having a new distance d_0' as seen in (30b). Therefore, the model median PL is given by (29):

$$PL_b$$
$$= \begin{cases} 20\log \left(\frac{4\pi d_0}{\lambda} \right), & \text{for } d \leq d_0' \\ A + 10\gamma \log \left(\frac{d}{d_0} \right) + \Delta L_{bf} + \Delta L_{bh}, & \text{for } d > d_0' \end{cases}$$
$$(29)$$

where A, d_0', γ, ΔL_{bf} (frequency correction factor) and ΔL_{bh} (MS antenna height correction factor) are defined using (30a) through (30e) as:

$$A = 20\log\left(\frac{4\pi d_0'}{\lambda}\right) \tag{30a}$$

$$d_0' = d_0 10^{-\left(\frac{\Delta L_{bf} + \Delta L_{bh}}{10\gamma}\right)} \tag{30b}$$

$$\gamma = a - bh_{te} + \frac{c}{h_{te}} \tag{30c}$$

$$\Delta L_{bf} = 6.0\log\left(\frac{f}{2000}\right) \tag{30d}$$

$$\Delta L_{bh} = \begin{cases} -10\log\left(\frac{h_{re}}{3}\right), & for\ h \le 3m \\ -20\log\left(\frac{h_{re}}{3}\right), & for\ h > 3m \end{cases} \tag{30e}$$

The SUI Model Parameters (Table 3) are used to calculate the parameters *a, b, c,* and d_0 of the model.

H. LEE PROPAGATION MODEL

The model was first proposed by William C. Y. Lee in 1982 [59]. The model quickly became widely used among wireless system engineers and researchers due to its great accuracy in propagation prediction [60], as well as tuning of the model parameters for different local environments by additional field measurements [12]. AMPS, DAMPS, IS-95, PCS, are a few systems designed by using the model. The model algorithm is fast and simple with distance, transmit power, antenna height, and frequency values as the inputs to the model. It is a modified power-law model that has antenna height and frequency correction factors which can easily be customized for the different environment [61]. Generally, the model is composed of two parts. Part one is an area-to area prediction and is useful for the prediction of PL typically over a flat terrain leaving out the configuration of the terrain. It is important to note that in hilly regions, the area-to-area prediction becomes inadequate. On the other hand, the second part still makes use of the area-to-area prediction as a base and added the capability of point-to-point prediction, to solve the problem due to hilly regions. Large errors do arise due to the application of the model in a non-terrain.

The model was designed to operate at 900 MHz frequency [78] but does include a frequency adjustment factor which is useful for analytically increasing the frequency range [79]. For the area-to-area prediction, a 1 km range is used as reference median PL illustrated as L_o, the slope of the PL curve γ in dB, and adjustment factor F_0. The median PL at distance d, is given by (31)

$$PL_{Lee}(d) = L_o + \gamma \log_{10} d - 10 \log_{10} F_0 \tag{31}$$

The adjustment factor F_0 comprises of several factors which are illustrated as (32):

$$F_0 = F_1 F_2 F_3 F_4 F_5 \tag{32}$$

where F_1 represents the correction factor for BS antenna height, the respective correction factors for the base station

antenna height (h_{te}), F_2 is the BS antenna gain (G_{te}), correction factor, F_3 is the MS antenna height (h_{re}), correction factor, F_4 is the frequency (f) adjustment factor, and the F_5 represent the MS antenna gain (G_{re}) correction factor. The values are as in [80] and shown in (33a)-(33e) as:

$$F_1 = \left(\frac{h_{te}\,(m)}{30.48}\right)^2 = \left(h_{te}\left(\frac{ft}{100}\right)\right)^2 \tag{33a}$$

$$F_2 = \frac{G_{te}}{4} \tag{33b}$$

$$F_3 = \begin{cases} \left(\frac{h_{re}\,(m)}{3}\right)^2, & if\ h_m\,(m) > 3 \\ \left(\frac{h_{re}\,(m)}{3}\right), & if\ h_m\,(m) < 3 \end{cases} \tag{33c}$$

$$F_4 = \left(\frac{f}{900}\right)^{-n} \quad for\ 2 < n < 3 \tag{33d}$$

$$F_5 = \frac{1}{G_{re}} \tag{33e}$$

where G_{re} represent the antenna receiver gain relative to a halfwave dipole.

The computation of the reference PL along a range of 1 km is given in (34)

$$L_0 = G_{te} + G_{re} + 20(\log \lambda - \log d) - 22 \tag{34}$$

where λ is the wavelength in meters.

For the point-to-point prediction, the PL is given by (35)

$$PL_{Lee}(d) = L_o + \gamma \log_{10} d - 10\left(\log_{10} F_0 - 2\log \times \left(\frac{H_{ET}}{30}\right)\right) \tag{35}$$

where H_{ET}, is the effective height of the terrain in meters.

I. EGLI PATH LOSS MODEL

The model was derived by Egli [81], [82] based on the acquired real data of Ultra-high frequency (UHF) and Very high frequency (VHF) transmissions in numerous large cities. It is a terrain model for radiofrequency propagation at a frequency range of 90 MHz - 1GHz, suitable for mobile communication systems where LoS occurs between a fixed BS antenna and that of a mobile antenna [81], that is, more useful for LoS transmission. It applies to scenarios where signals are transmitted over irregular terrain. However, it is not suitable in terrain with vegetative obstructions. The PL is produced as a single quantity without subdividing the losses none consider the diffraction losses due to propagation over terrains that are irregular [83]. The model operates at distances less than 60 km [84]. The model PL [85] is given by (36a) for $h_{re} \le 10m$ and (36b) where $h_{re} \ge 10m$;

$$PL_{Egli} = 20\log(f_c) + 40\log(d) - 20\log(h_{te}) + 76.3 - 10\log(h_{re}) \tag{36a}$$

$$PL_{Egli} = 20\log(f_c) + 40\log(d) - 20\log(h_{te}) + 85.9 - 20\log(h_{re}) \tag{36b}$$

J. LOG-NORMAL SHADOWING MODEL

The log-distance path loss model [86] was derived as an extension of the Friis free space model, which is used for prediction of propagation loss for a wider area [87], [88]. Unfortunately, the log-distance path loss model does not consider the shadowing effects due to the changing degrees of clutter between the BS and the receiver [43]. It assumes the PL variations occurs exponentially with respect to distance, and the PL in dB is illustrated by (37):

$$\overline{PL}(d) = \overline{PL}(d_0) + 10n \log\left(\frac{d}{d_0}\right) \quad (37)$$

where d illustrates the transmitter and receiver separation distance in meters, n represents the path loss exponent (PLE), while d_0, is the close-in reference distance in meters, and usually at a distance close to the antenna of the transmitter, and outside the near field. $\overline{PL}(d_0)$, is obtained using the FSPL (3), while PLE differs due to environments, and it is calculated as given in (38) using empirical data.

$$n = \frac{PL(d) - PL(d_0)}{10 \log\left(\frac{(d)}{(d_0)}\right)} \quad (38)$$

On the other hand, the log-normal Shadowing Model accounted for the shadowing effect of the signal transmission, by adding X, a zero-mean Gaussian random variable with standard deviation σ expressed in dB as given in the (39). This model is a log-normal distribution (Gaussian distribution about the distance-dependent mean of the equation), which defines the random shadowing effects that ensue over numerous measurement locations with the same BS and MS separation distance but with diverse levels of clutter on the path of propagation [89].

$$PL(d) = PL(d_0) + 10n \log\left(\frac{d}{d_0}\right) + X_\sigma \quad (39)$$

where $PL(d_0)$ represents the reference PL measured at the reference distance d_0, n is PLE and X_σ, is the shadowing effects. Furthermore, the n value is dependent on the specific propagation of the environment. Table 5 illustrates a typical PLE value acquired in the mobile communications environment [90]:

TABLE 5. Typical path loss exponent values [90].

Environment	Path Loss Exponent (n)
Free space	2
Urban area cellular radio	2.7 to 3.5
Shadowed urban cellular radio	3 to 5
Inside a building - line-of-sight	1.6 to 1.8
Obstructed in building	4 to 6
Obstructed in factory	2 to 3
Free space	2

Other research such as [91] had suggested the application of the log-normal shadowing model with two different slopes as well as deviation values. The breakpoint distance d_b,

separates the two slopes of the model. The experiment indicated a superior prediction accuracy of the two slopes logs normal model near ground scenarios. Equation (40) expresses the model as:

$$PL(d_i)$$
$$= \begin{cases} PL(d_b) + 10n_1 \log\left(\frac{d_i}{d_b}\right) + X_{\sigma 1}, & d_i \le d_b \\ PL(d_{b+1}) + 10n_2 \log\left(\frac{d_i}{d_{b+1}}\right) + X_{\sigma 2}, & d_i > d_b \end{cases} \quad (40)$$

Generally, in the case of LOS scenarios, the breakpoint distance is estimated as given by (41):

$$d_b = \frac{4h_{re}h_{te}}{\lambda} \quad (41)$$

The descriptions of the two slopes are done before and after the breakpoint d_b, which are usually determined by measurements carried out close to the transmitter. Likewise, the selection of the reference PL ($PL(d_b)$, and $PL(d_{b+1})$) were done before and after the breakpoint, respectively.

K. BLOCKED LoS (NLoS) MODEL

This model was the first to be reviewed for mmWave frequencies by [92]. The model modified the FSPL by accounting for shadow loss as a result of obstructions with the addition of attenuation of 25dB [93]. The model is considered a simple model since the possible losses were easily accounted for by the addition of a constant parameter. The PL model in dB is expressed by (42):

$$\overline{PL}(d) = 20 \log d + 20 \log f + 20 \log\left(\frac{4\pi}{0.3}\right) + 25 \quad (42)$$

L. 3RD GENERATION PARTNERSHIP PROJECT (3GPP)
1) SPATIAL CHANNEL MODEL (SCM)

This model was developed in 2011 by 3GPP for cellular MIMO system [94] for the frequency range 1 GHz to 3 GHz. The model considered three scenarios including Suburban Macrocell (SMa), Urban Macrocell (UMa) both for BS and MS distance of 3 km, and Urban Microcell (UMi) for BS and MS distance of 1 km. The SMa and UMa scenarios took an assumption that the BS antenna heights are above that of rooftop height. While the UMi assumed that the BS antenna and that of the rooftop are the same. The PL models for the three scenarios are as follows:

The COST 231 Hata urban model was modified for SMa and UMa as given in (43):

$$PL = (44.9 - 6.55 \log(h_{te})) \log\left(\frac{d}{1000}\right) + 45.5$$
$$+ (35.46 - 1.1h_{re}) \log f - 13.82 \log h_{te} + 0.7h_{re} + C_m$$
$$C_m = \begin{cases} 0\ dB & \text{for SMa} \\ 3\ dB & \text{for Uma} \end{cases} \quad (43)$$

where h_{te}, h_{re}, f, d are as stated previously. C is a constant factor

The COST 231 Walfish-Ikegami model was modified for both the UMi NLoS and UMi LoS model with the following parameters: 12.5m h_{te}, building height 12m, the distance between buildings is 50m, street width 25m, 1.5m h_{re}. The PL models are given in (44) and (45) respectively:

$$PL = -55.9 + 38^* \log d + \left(24.5 + 1.5^* \frac{f}{925}\right)^* \log f \tag{44}$$

$$PL = -35.4 + 26^* \log d + 20^* \log f \tag{45}$$

2) 3GPP TR 36.873

3GPP took a study on the 3D channel model for 4G (LTE) [95] for the frequency range 2 GHz – 6 GHz for such scenarios as three-dimension Urban Microcell (3D-UMi) that has a high density of MS and BS is lower than surrounding structures. Three-dimension Urban Macrocell (3D-UMa) also with a high density of MS, but the BS is taller than the structures. Three-dimension Urban Macrocell (3D-UMa-H) which has a high density of high-rise structures. Indoor Hotspot cell (3D-InH). The BS height varies between 10m to 35m while the MS height differs too. The distribution of the shadow fading (SF) is log-normal, and its standard deviation for each scenario. Figure 3 indicates the distance definition:
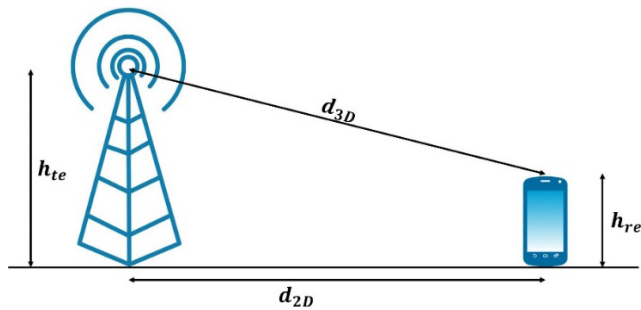

FIGURE 3. Distance definition of d_{2D} and d_{3D} for outdoor models.

The models are further divided using the separation between the BS (h_{te}) and MS (h_{re}), usually with the range of 10m, d'_{BP} and 5000m. Breakpoint distance (d'_{BP}) was defined by [96], [97], and given by (46a). The PL for the various scenarios is expressed as:

$$d'_{BP} = 4h'_{te}h'_{re}\frac{f\,[GHz]}{c} \tag{46}$$

$$h'_{te} = h_{te} - 1m \tag{46a}$$

$$h'_{re} = h_{re} - 1m \tag{46b}$$

where c is the speed of light, h'_{te}, and h'_{re}, are the effective antenna heights at the BS and the MS, respectively.

For the 3D-UMi (LoS)

$$PL_1 = 22\log(d_{3d}) + 28 + 20\log(f) \tag{47}$$

where σ_{SF} is 3, distance range is $10m < d_{2D} < d'_{BP}$ and default values for BS (h_{te}) and MS (h_{re}) is 10m and

$1.5m \leq h_{re} \leq 22.5m$ respectively, and

$$PL_2 = 40\log(d_{3D}) + 28 + 20\log(f) - 9\log((d'_{BP})^2 + (h_{te} - h_{re})^2) \tag{48}$$

where σ_{SF} is 3dB, distance range is $d'_{BP} < d_{2D} < 5000m$ and default values for BS (h_{te}) and MS (h_{re}) is 10m and $1.5m \leq h_{re} \leq 22.5m$ respectively.

For the 3D-UMi (NLoS) (hexagonal cell Layout)

$$PL = max\left(PL_{3D-UMi-NLOS}, PL_{3D-UMi-LOS}\right)$$

$$PL_{3D-UMi-NLOS} = 36.7\log(d_{3D}) + 22.7 + 26\log f - 0.3(h_{re} - 1.5) \tag{49}$$

where σ_{SF} is 4, distance range is $d'_{BP} < d_{2D} < 2000m$ and antenna height default values for BS (h_{te}) and MS (h_{re}) is 10m and $1.5m \leq h_{re} \leq 22.5m$ respectively.

For the 3D-UMa (LoS), the PL model is the same with 3D-UMi (LoS) but with different parameter values, as stated in (50) and (51).

$$PL_1 = 22\log(d_{3d}) + 28 + 20\log(f) \tag{50}$$

where σ_{SF} is 4, distance range is $10m < d_{2D} < d'_{BP}$, default values for BS (h_{te}) and MS (h_{re}) is 25m and $1.5m \leq h_{re} \leq 22.5m$ respectively.

$$PL_2 = 40\log(d_{3D}) + 28 + 20\log(f) - 9\log((d'_{BP})^2 + (h_{te} - h_{re})^2) \tag{51}$$

where σ_{SF} is 4, distance range is $d'_{BP} < d_{2D} < 5000m$, default values for BS (h_{te}) and MS (h_{re}) is 10m and $1.5m \leq h_{re} \leq 22.5m$ respectively.

For the 3D-UMa (NLoS)

$$\begin{aligned}PL_{NLOS} = {} & 161.04 - 7.1\log(W) + 7.5\log(h) \\ & - \left(24.37 - 3.7\left(\frac{h}{h_{te}}\right)^2\right)\log h_{te} \\ & + (43.42 - 3.1\log h_{te})(\log(d_{3D}) - 3) \\ & + 20\log f - \left(3.2(\log 17.625)^2 - 4.97\right) \\ & - 0.6(h_{re} - 1.5)\end{aligned} \tag{52}$$

where σ_{SF} is 6, distance range is $10 < d_{2D} < 5000m$ and antenna height default values for BS (h_{te}) and MS (h_{re}) is 25m and $1.5m \leq h_{re} \leq 22.5m$ respectively. h (average building height) is 20m, W (street width) is 20m. Applicability ranges are $5m < h < 50m$, $5m < W < 50m$, $10m < h_{te} < 150m$, $1m < h_{re} < 10m$

For the 3D-RMa (LoS)

$$\begin{aligned}PL_1 = {} & 20\log\left(\frac{40\pi d_{3D}f}{3}\right) \\ & + min\left(0.03h^{1.72}, 10\right)\log(d_{3D}) \\ & - min\left(0.044h^{1.72}, 14.77\right) + 0.002\log(h)d_{3D}\end{aligned} \tag{53}$$

$$PL_2 = PL_1(d_{3D}) + 40\log\left(\frac{d_{3D}}{d_{BP}}\right) \tag{54}$$

where $DV = \begin{cases} PL_1, 4dB\,(\sigma_{SF})\,,10m < d_{2D} < d_{BP} \\ PL_2, 6dB\,(\sigma_{SF})\,,d_{BP} < d_{2D} < 5000m \end{cases}$,
the distance range is $10 < d_{2D} < 5000m$ and antenna height default values for BS (h_{te}) and MS (h_{re}) is 35m and 1.5m, respectively. h (average building height) is 20m, W (street width) is 5m. Applicability ranges are $5m < h < 50m$, $5m < W < 50m$, $10m < h_{te} < 150m$, $1m < h_{re} < 10m$. The Breakpoint distance for 3D-RMa (LoS) is given as (52a)

$$d_{BP} = \frac{2\pi h_{te} h_{re} f}{c} \tag{54a}$$

For the 3D-RMa (NLoS)

$$PL = 161.04 - 7.1\log(W) + 7.5\log(h)$$
$$- \left(24.37 - 3.7\left(\frac{h}{h_{te}}\right)^2\right)\log h_{te}$$
$$+ (43.42 - 3.1\log h_{te})(\log(d_{3D}) - 3)$$
$$+ 20\log f - \left(3.2(\log 11.75 h_{re})^2 - 4.97\right) \tag{55}$$

where σ_{SF} is 8, distance range is $10 < d_{2D} < 5000m$ and antenna height default values for BS (h_{te}) and MS (h_{re}) is 35m and 1.5m, respectively. h (average building height) is 5m, W (street width) is 20m. Applicability ranges are $5m < h < 50m$, $5m < W < 50m$, $10m < h_{te} < 150m$, $1m < h_{re} < 10m$.

3) 3GPP TR 38.901

3GPP took another study on channel modelling [98] for frequency range 0.5 GHz – 100 GHz for such scenarios like Urban Microcell (UMi)-street canyon or open area is similar to the 3D-Umi scenario. The intension of the UMi is to capture real-life scenarios of a city. Urban Macrocell (UMa) is also comparable to the 3D-UMa scenario and indoor scenarios. As earlier said, the distribution of the σ_{SF} is log-normal, and its standard deviation for each scenario. Figure 3 indicate the distance definition as show above. The break point distance d'_{BP}, d_{BP}, h'_{te} and h'_{re} are as described above. The PL models for the various scenarios is expressed as:

For UMi-street canyon (LoS)

$$PL_1 = 32.4 + 21\log(d_{3D}) + 20\log(f_c) \tag{56}$$
$$PL_2 = 32.4 + 40\log(d_{3D}) + 20\log f - 9.5\log\left((d'_{BP})^2 + (h_{te} - h_{re})^2\right) \tag{57}$$

where $PL_{UMi-LOS} = \begin{cases} PL_1, 10m \le d_{2D} \le d'_{BP} \\ PL_2, d'_{BP} \le d_{2D} \le 5000 \end{cases}$, $\sigma_{SF} = 4.0$, the frequency range is $0.5 < f < 100GHz$ and antenna height default values for BS (h_{te}) and MS (h_{re}) is 10m and $1.5m \le h_{UE} \le 22.5m$ respectively.

For UMi-street canyon (NLoS)

$$PL_{UMi-NLOS} = max\left(PL_{UMi-LOS}, PL'_{UMi-NLOS}\right)$$
$$PL'_{UMi-NLOS} = 35.3\log(d_{3D})$$
$$+ 22.4 + 21.3\log f - 0.3(h_{re} - 1.5) \tag{58}$$

where σ_{SF} is 7.82, distance range is $10 < d_{2D} < 5000m$ and antenna height default values for BS (h_{te}) and MS (h_{re}) is 10m and $1.5m \le h_{re} \le 22.5m \le$ respectively.

Optional PL with 1m reference distance

$$PL = 32.4 + 20\log f + 31.9\log(d_{3D}) \tag{59}$$

where σ_{SF} is 8.2.

For the 3GPP UMa (LoS)

$$PL_1 = 28.0 + 22\log(d_{3D}) + 20\log(f_c) \tag{60}$$
$$PL_2 = 28 + 40\log(d_{3D}) + 20\log f - 9\log\left((d'_{BP})^2 + (h_{te} - h_{re})^2\right) \tag{61}$$

where $PL_{UMi-LOS} = \begin{cases} PL_1, 10m \le d_{2D} \le d'_{BP} \\ PL_2, d'_{BP} \le d_{2D} \le 5000 \end{cases}$, $\sigma_{SF} = 4.0$, the frequency range is $0.5 < f < 100GHz$ and antenna height default values for BS (h_{te}) and MS (h_{re}) is 25m and $1.5m \le h_{UE} \le 22.5m$ respectively.

For the 3GPP UMa (NLoS)

$$PL_{UMi-NLOS} = max\left(PL_{UMi-LOS}, PL'_{UMi-NLOS}\right)$$
$$PL'_{UMi-NLOS} = 13.54 + 39.08\log(d_{3D})$$
$$+ 20\log f - 0.6(h_{re} - 1.5) \tag{62}$$

where σ_{SF} is 6, distance range is $10 < d_{2D} < 5000m$ and antenna height default values for BS (h_{te}) and MS (h_{re}) is 25m and $1.5m \le h_{re} \le 22.5m \le$ respectively.

Optional PL with 1m reference distance

$$PL = 32.4 + 20\log f + 30\log(d_{3D}) \tag{63}$$

where σ_{SF}, is 7.8.

The model lacks measurement validation in some cases [96].

M. 5G CHANNEL MODEL (5GCM)

This model was derived based on extensive measurement campaigns as well as ray tracing results of other multiple 3D channel models by a collaboration of universities and 15 companies [99]. The study provided some extensibility to the 3GPP TR 36.873 models [95] by accommodating a higher frequency range up to 100 GHz as well as channel bandwidths in the range of 100 MHz to 2 GHz, other requirements for the new 5G channel model are discussed in [99]. The model was developed for a selective set of 5G scenarios such as Urban Micro (UMi) Street Canyon and Open Square with outdoor-to-outdoor (O2O) and outdoor-to-indoor (O2I), Urban Macro (UMa) with O2O and O2I, and the Indoor (InH) - Open and closed Office, Shopping Malls. The scenario descriptions are similar to those of the 3GPP.

The model considered three PL models namely the close-in (CI) free space reference distance PL model [100]–[102] the close-in free space reference distance model with frequency-dependent path loss exponent (CIF) [103], and the Alpha-Beta-Gamma (ABG) PL model [46], [103]–[105]. The PL models for the various scenarios at frequency range $6GHz < f < 100GHz$ are expressed as follow:

For the 5GCM UMi-street canyon (LoS)

$$PL = 32.4 + 21\log(d_{3D}) + 20\log(f) \qquad (64)$$

Using the CI model with 1m reference distance and where σ_{SF} is 3.76

For 5GCM UMi-Street canyon NLoS

$$PL_1 = 32.4 + 31.7\log(d_{3D}) + 20\log(f) \qquad (65)$$

Using the CI model with 1m reference distance and where σ_{SF} is 8.09

$$PL_2 = 32.4\log(d_{3D}) + 22.4 + 21.3\log(f) \qquad (66)$$

Using the ABG model and where σ_{SF} is 7.82

5GCM UMi-Open Square LoS

$$PL_1 = 32.4 + 28.9\log(d_{3D}) + 20\log f \qquad (67)$$

Using the CI model with 1m reference distance and where σ_{SF} is 7.1

$$PL_2 = 41.4\log(d_{3D}) + 3.66 + 24.3\log f \qquad (68)$$

Using the ABG model and where σ_{SF}, is 7.0.

N. METIS MODEL

Mobile and Wireless Communications Enablers for the Twenty-twenty Information Society is a European Union-sponsored research project [106]. The model consists of a stochastic, map-based, hybrid model (derived from both stochastic and map-based model) in the provision of a scalable channel model, and it was developed based on the 3D ray-tracing principles [107]. The model accommodated propagation scenarios such as UMi and UMa (O2O, O2I), RMa, Indoor, Highway for frequency ranges of 0.8 to 60 GHz. The METIS adapted some existing models for most of these various scenarios, as stated in Table 7-1 of [106]. Some of the models comprise breakpoints distance d_{BP} based on sub-6 GHz work [96]. A scaling factor is used for the LoS scenarios, therefore, the d_{BP} (m) is given in (69):

$$d_{BP} = 0.87 \exp\left(-\frac{\log f}{0.65}\right)\frac{4(h_{te}-1m)(h_{re}-1m)}{\lambda} \qquad (69)$$

The ITU-R UMi path loss model was modified to derive the METIS UMi model that covers a radio frequency range from 0.8 to 60 GHz. Other parameters like the power decay constant before and after the breakpoint, n_1 and n_2 are 2.2 and 4.0 respectively, while the σ_{SF} is 3.1 and the PL_0 is the PL offset given by (70).

$$PL_0 = -13.8\log f + 3.34 \qquad (70)$$

Therefore, the modified PLs are given as:

$$PL_1(d_1) = 10n_1\log(d_1) + 28 + 20\log f + PL_0 \qquad (71)$$

For $10m < d \leq d_{BP}$, frequency range $0.8 < f < 60GHz$, σ_{SF} is 3.1, h_{te} is 10m, and $1.5m \leq h_{re} \leq 22.5m$ and

$$PL_2(d_1) = 10n_2\log(d_1) + 7.8 - 18\log(h_{te}h_{re})$$
$$+2\log f + PL_0(d_{BP}) \qquad (72)$$

For $d_{BP} < d \leq 500m$, frequency range $0.8 < f < 60GHz$, σ_{SF} is 3.1, h_{te} is 10m, and $1.5m \leq h_{re} \leq 22.5m$

For the METIS UMi model NLoS model:

$$PL = \max(PL_{UMi-LOS}(d_{3D}), PL_{UMi-NLOS}(d_{3D}))$$
$$PL_{NLOS} = 36.7\log_{10}(d_{3D}) + 23.15 + 26\log_{10}(f) - 0.3(h_{re}) \qquad (73)$$

For $10m < d_{2D} \leq 2000m$, frequency range $0.45 < f < 6GHz$, σ_{SF} is 4.0, h_{te} is 10m, and $1.5m \leq h_{re} \leq 22.5m$.

O. IMT–ADVANCED CHANNEL MODEL

The model was released in 2009 by the ITU-R [108], which accommodates a frequency range of 2 GHz to 6 GHz. The model is based on WINNER models. The PL model was derived for propagation scenarios such as InH, UMi, UMa, and RMa by conducting measurement campaigns with references to [109]–[113] and also results from the literature. For the Rural scenario, the model is applicable for the frequency range from 450 MHz to 6 GHz. The PL models for various scenarios are given as:

For IMT-UMi LoS

$$PL_1 = 22.\log(d) + 28.0 + 20\log(f) \qquad (74)$$
$$PL_2 = 40\log(d_1) + 7.8 - 18\log(h'_{te}) - 18\log(h'_{re})$$
$$+2\log(f) \qquad (75)$$

where $PL_{LOS} = \begin{cases} PL_1, 10m \leq d_1 \leq d'_{BP} \\ PL_2, d'_{BP} \leq d_1 \leq 5000 \end{cases}$, σ_{SF} is 3 for both, the frequency range is $2 < f < 6GHz$ and antenna height default values for BS (h_{te}) and MS (h_{re}) is $10m$ and $1.5m$, respectively.

For IMT-UMi NLoS

Manhattan grid layout:

$$PL = \min(PL(d_1, d_2), PL(d_2, d_1)) \qquad (76)$$

where

$$PL(d_k, d_l) = PL_{LOS}(d_k) + 17.9 - 12.5n_j$$
$$+10n_j\log(d_l) + 3\log f \qquad (76a)$$

And

$$n_j = \max(2.8 - 0.0024d_k, 1.84) \qquad (76b)$$

Note that the PL is applied when $0 < \min(d_1, d_2) < \frac{w}{2}$ For $10m < d_1 + d_2 \leq 5000m$, frequency range $2 < f < 6GHz$, σ_{SF} is 4.0, h'_{te} is 10m, and h_{re} is 1.5m, $\frac{w}{2} < \min(d_1, d_2)$ is 20 m (street width)

Hexagonal cell layout:

$$PL = 36.7\log(d) + 22.7 + 26\log f \qquad (77)$$

For $10m < d \leq 2000m$, frequency range $2 < f < 6GHz$, σ_{SF} is 4.0, h_{te} is 10m, and h_{re}, is 1-2.5m.

For IMT-UMa LoS

The PL models are the same with the IMT-UMi LoS but with different parameter values which are σ_{SF} is 4.0 for both and the default values for BS (h_{te}) is 25m while h_{re} remain 1.5m

For IMT-UMa NLoS

The 3GPP 3D-RMa NLoS PL model was adopted here but with σ_{SF} as 6.0, h_{te} as 25m, h (average building height) as 20m. the applicability ranges remain the same also.

For IMT-SMa LoS

The 3GPP 3D-RMa (LoS) was adopted but h as10m, W as 20m, all other parameter values and applicability ranges remain the same.

For IMT-SMa (NLoS)

The 3GPP 3D-RMa (NLoS) was adopted but with h as 10m, all other parameter values and applicability ranges remain the same.

For the IMT-RMa (LoS)

The 3GPP 3D-RMa (LoS) was adopted but with $d_{BP} \leq d \leq 10000m$, while the applicability ranges of h, W, h_{te} and h_{re} are the same as the 3D UMa NLoS.

For the IMT-RMa (NLoS)

The 3GPP 3D-RMa (NLoS) was adopted with all the parameter values, and applicability ranges remain the same.

P. mmMAGIC

In July 2015, the European Commission's 5G Public-Private Partnership (PPP) program sponsored a project known as Millimeter–Wave Based Mobile Radio Access Network for Fifth Generation Integrated Communications (mmMAGIC) [114] intending to develop an ideal concept for mobile. The scenarios are consistent with that of the 5GCM or 3GPP models but with the addition of Indoor, Airport, stadium, and Metro station.

For mmMAGIC UMi-Street canyon LoS, the ABG PL model was adapted, but the parameter values are different. The PL is given by (78) as:

$$PL = 19.2log(d_{3D}) + 32.9 + 20.8log(f_c) \qquad (78)$$

where σ_{SF} is 2.0, and the frequency range of $6 < f < 100GHz$

For mmMAGIC UMi-Street canyon NLoS;

$$PL = 45.0log(d_{3D}) + 31.0 + 20.0log(f_c) \qquad (79)$$

where σ_{SF}, is 7.82, and frequency range $6 < f < 100GHz$

Q. MiWEBA

The Millimeter-Wave Evolution for Backhaul and Access (MiWEBA) [115] project was a 3D channel model instituted for the 60 GHz frequency band that will be proficient at supporting beamforming at the transmitter and addressing other different challenges. Such challenges as spatial consistency, shadowing, environment dynamics, antenna polarization. The research focused more on device-to-device (D2D),

backhaul, mobile access (University campus, street canyon, hotel lobby) [98], [116]. The model is a combination of measurement-based parameters and other existing models, making it a hybrid model. The street canyon access PL model is given by (80) as:

$$PL = \alpha + n10\log\left(\frac{d}{d_0}\right) \qquad (80)$$

where PL_0 is 82.02dB, n is 2.36 and d_0 is 5m

R. WINNER CHANNEL MODELS
1) WINNER I
The Wireless World Initiative New Radio (WINNER) initiated a project known as WINNER Work Package 5 (WP5) intending to model a wideband multiple-input multiple-output (MIMO) channel at 5 GHz frequency range. Measurement campaigns were performed at 2 and 5 GHz for multiple scenarios such as UMi, UMa, RMa, SMa, small indoor office, and stationary feeder links [117]. The derived WINNER PL model has a form as given in (81), where A includes the PLE parameter and parameter B is the intercept. The derived PL models for various scenarios are as:

$$PL_{WI} = A\log(d) + B \qquad (81)$$

Therefore, for the WINNER I-UMi (LoS):

$$PL = 22.7log(d\,[m]) + 41.0 \qquad (82)$$

where σ_{SF} is 2.3 and applicability range of $10m < d < 650m$.

For the WINNER I-UMi (NLoS):

$$PL = 0.096(d_1\,[m]) + 65 + (28 - 0.024d_1\,[m])\,log(d_2\,[m]) \qquad (83)$$

where σ_{SF} is 3.1 and applicability range of $10m < d_1 < 550m$ and $\frac{w}{2} < d_2 < 450m$. w is the LoS street width, d_1 *is distance along main street*, and d_2, is the perpendicular street distance.

For the WINNER I-SMa (LoS):

$$PL_1 = 23.8log(d) + 41.6 \qquad (84)$$
$$PL_2 = 40.0\log\left(\frac{d}{d_{BP}}\right) + 41.6 + 23.8\log(d_{BP}) \qquad (85)$$

where the applicability range and σ_{SF} are

$$\begin{cases} PL_1, & 30m \leq d \leq d_{BP}, \sigma_{SF} \text{ is } 4 \\ PL_2, & d_{BP} \leq d \leq 5000, \sigma_{SF} \text{ is } 6 \end{cases}$$

and h_{te} is 11.7m

For the WINNER I-SMa (NLoS)

$$PL = 40.2\log(d\,[m]) + 27.7 \qquad (86)$$

where σ_{SF} is 8.0 and applicability range of $50m < d < 5000m$

For the WINNER I-UMa (NLoS)

$$PL = 35.0log(d\,[m]) + 38.4 \qquad (87)$$

where σ_{SF} is 8.0 and applicability range of $50m < d < 5000m$

For the WINNER I-RMa (LoS)

$$PL_1 = 21.5 log(d\,[m]) + 44.6 \qquad (88)$$

$$PL_2 = 40.0 \log\left(\frac{d}{d_{BP}}\right) + 44.6 + 21.5 \log(d_{BP}) \quad (89)$$

where the applicability range and σ_{SF} are

$$\begin{cases} PL_1, & 30m \le d \le d_{BP}, \sigma_{SF} \text{ is } 3.5 \\ PL_2, & d_{BP} \le d \le 10km, \sigma_{SF} \text{ is } 6 \end{cases}$$

and h_{te} is 19 - 25m

For the WINNER I-RMa (LoS)

$$PL = 25.1 \log(d\,[m]) + 55.8 \qquad (90)$$

where σ_{SF} is 8.0 and applicability range of $30m < d < 10km$

2) WINNER II

The aim of the WINNER II [118] was to develop a sole ubiquitous RAT that will be adaptable to various scenarios of mobile communication systems. The concept of channel modelling of WINNER I was optimized in WINNER II to set new multidimensional channel models with extended frequency ranges as well as a broader propagation scenario. The propagation scenarios include bad Umi, indoor-to-outdoor (I2O), bad UMa, O2I, BS feeder link to fixed relay station (FRS), and moving networks BS to mobile relay station (MRS), MRS to the mobile station (MS).

The PL models for the different scenarios were developed based on measurement campaigns and open literature results. The models are applicable within the frequency range from $2 - 6$ GHz as well as various antenna heights. The derived WINNER PL model has a form as given in (91).

$$PL_{WII} = A \log(d\,[m]) + B + C \log\left(\frac{f}{5.0}\right) + X \quad (91)$$

where A is inclusive of PLE, B is the intercept, C illustrates the PL frequency dependence, and X is an optional, environment-specific term, and the free space PL used is given as (92), and the derived PL models for various scenarios are shown in the subsequent s as;

$$PL_{free} = 20 \log(d) + 46.4 + 20 \log\left(\frac{f}{5.0}\right) \qquad (92)$$

For the WINNER II-UMi (LoS):

$$PL_1 = 22.7 \log(d\,[m]) + 41 + 20 \log\left(\frac{f}{5.0}\right) \qquad (93)$$

$$PL_2 = 40.0 \log(d_1) + 9.45 - 17.3 \log\left(h'_{te}\right)$$
$$- 17.3 \log\left(h'_{re}\right) + 2.7 \log\left(\frac{f_c}{5.0}\right) \qquad (94)$$

where the applicability range and σ_{SF} are

$$\begin{cases} PL_1, & 10m \le d_1 \le d'_{BP}, \sigma_{SF} \text{ is } 3 \\ PL_2, & d'_{BP} \le d_1 \le 5000, \sigma_{SF} \text{ is } 3, \end{cases}$$

h_{te} is 10m and h_{re} is 1.5m

For the WINNER II-UMi and WINNER II Bad-UMi (NLoS):

$$PL = \min\left(PL\,(d_1, d_2), PL\,(d_2, d_1)\right) \qquad (95)$$

where

$$PL = (d_k, d_l) = PL_{LOS}\,(d_k) + 20 - 12.5n_j$$
$$+ 10n_j \log(d_1) + 3 \log\left(\frac{f_c}{5.0}\right) \qquad (95a)$$

and $n_j = \max(2.8 - 0.0024d_k, 1.84)$, PL_{LOS} is WINNER II-UMi (LoS) scenario, $k, l\epsilon\{1, 2\}$, σ_{SF} is 4, applicability range of $10m < d_1 < 5000m$ and $\frac{w}{2} < d_2 < 2000m$. w is 20 m (street width), h_{te} is 10m and h_{re} is 1.5m when $0 < d_2 < w/2$.

For WINNER II-SMa (LoS):

$$PL_1 = 23.8 \log(d\,[m]) + 41.2 + 20 \log\left(\frac{f}{5.0}\right) \quad (96)$$

$$PL_2 = 40.0 \log(d_1) + 11.65 - 16.2 \log(h_{te})$$
$$- 16.2 \log(h_{re}) + 3.8 \log\left(\frac{f_c}{5.0}\right) \qquad (97)$$

where the applicability range and σ_{SF} are

$$\begin{cases} PL_1, & 30m \le d \le d'_{BP}, \sigma_{SF} \text{ is } 4 \\ PL_2, & d_{BP} \le d \le 5000, \sigma_{SF} \text{ is } 6, \end{cases}$$

h_{te} is 25m and h_{re} is 1.5m

For WINNER II-SMa (NLoS):

$$PL = (44.9 - 6.55 \log(h_{te})) \log(d) + 31.46$$
$$+ 5.83 \log(h_{te}) + 23 \log\left(\frac{f_c}{5.0}\right) \qquad (98)$$

where σ_{SF} is 8, applicability range of $50m < d < 5000m$, h_{te} is 25m, and h_{re}, is 1.5m.

For WINNER II-UMa (LoS):

$$PL_1 = 26 \log(d\,[m]) + 39 + 20 \log\left(\frac{f}{5.0}\right) \qquad (99)$$

$$PL_2 = 40.0 \log(d_1) + 13.47 - 14.0 \log(h_{te})$$
$$- 14.0 \log(h_{re}) + 6.0 \log\left(\frac{f_c}{5.0}\right) \qquad (100)$$

where the applicability range and σ_{SF} are

$$\begin{cases} PL_1, & 10m \le d \le d'_{BP}, \sigma_{SF} \text{ is } 4 \\ PL_2, & d'_{BP} \le d \le 5000, \sigma_{SF} \text{ is } 6, \end{cases}$$

h_{te} is 25m and h_{re} is 1.5m

For WINNER II-UMa and WINNER II Bad-UMa (NLoS):

$$PL = (44.9 - 6.55 \log(h_{te})) \log(d) + 34.46$$
$$+ 5.83 \log(h_{te}) + 23 \log\left(\frac{f_c}{5.0}\right) \qquad (101)$$

where σ_{SF} is 8, applicability range of $50m < d < 5000m$, h_{te} is 25m, and h_{re}, is 1.5m.

For WINNER II-RMa and Moving Network (LoS):

$$PL_1 = 21.5 \log (d\,[m]) + 44.2 + 20 \log \left(\frac{f}{5.0} \right) \quad (102a)$$

$$PL_2 = 40.0 \log (d_1) + 10.5 - 18.5 \log (h_{te})$$
$$- 18.5 \log (h_{re}) + 1.5 \log \left(\frac{f_c}{5.0} \right) \quad (102b)$$

where the applicability range and σ_{SF} are

$$\begin{cases} PL_1, & 10m \leq d \leq d_{BP}, \sigma_{SF} \text{ is } 4 \\ PL_2, & d_{BP} \leq d \leq 10km, \sigma_{SF} \text{ is } 6, \end{cases}$$

h_{te} is 25m and h_{re} is 1.5m

For WINNER II-RMa (NLoS):

$$PL = 25.1 \log (d) + 55.4 - 0.13 (h_{te} - 25) \log (d/100)$$
$$-0.9 (h_{re} - 1.5) + 21.3 \log \left(\frac{f_c}{5.0} \right) \quad (103)$$

where σ_{SF} is 8, applicability range of $50m < d < 5000m$, h_{te} is 32m, and h_{re}, is 1.5m.

The WINNER II PL models were based on measurement data obtained mainly from frequency range 2 and 5 GHz but were extended to $2 - 6$ GHz frequency range with the aid of PL frequency coefficient C.

3) WINNER +

The WINNER+ WP5 Channel models are an extension of the initial WINNER and WINNER II channel models. The channel model adopted the same Geometry-based Stochastic (GSCM) approach like that of the WINNER II models [119]. The model widens the application frequency ranges from 450 MHz to 6 GHz with up to 100 MHz RF bandwidth. The model is useful at the link level as well as the system-level evaluation performance.

The PL models for the different scenarios, such as the NLoS case hexagonal layout and Manhattan layout, were developed based on measurement campaigns and open literature results, leading to improving the zenith dimension parameters for the indoor, O2I (UMi and UMa), UMi, UMa, and SMa. The models are applicable within the frequency range from $0.45 - 6$ GHz, as well as various antenna heights. The derived WINNER PL models are given in the equations that follow as:

For the WINNER+ -UMi (LoS):

$$PL_1 = 22.7 log (d) + 27.0 + 20.0 \log (f) \quad (104)$$

$$PL_2 = 40.0 \log (d) + 7.56 - 17.3 \log \left(h'_{te} \right)$$
$$- 17.3 log \left(h'_{re} \right) + 2.7 \log f \quad (105)$$

where the applicability range and are

$$\begin{cases} PL_1, & 10m < d < d'_{BP} \\ PL_2, & d'_{BP} \leq d \leq 5km, \end{cases}$$

σ_{SF} is 3dB for both, h_{te} is 10m, and h_{re}, is 1.5m.

For Manhattan grid layout (NLoS):

$$PL = min (PL (d_1, d_2), PL (d_2, d_1)) \quad (106)$$

where

$$PL (d_k, d_l) = PL_{LOS} (d_k) + 17.3 - 12.5 n_j$$
$$+10 n_j \log (d_l) + 3 \log f \quad (106a)$$

And

$$n_j = max (2.8 - 0.0024 d_k, 1.84) \quad (106b)$$

For applicability range of $10m < d_1 < 5km$, $\frac{w}{2} < d_2 \leq 2km$, σ_{SF} is 4.0, h_{te} is 10m, and h_{re} is 1.5m, w is 20 m (street width). Note that the PL is applied when $0 < min (d_1, d_2) < \frac{w}{2}$ or hexagonal cell Layout (NLoS),

At Frequency range $0.45 - 1.5$ GHz

$$PL = (44.9 - 6.55 \log (h_{te})) \log (d) + 16.33$$
$$+5.83 \log (h_{te}) + 26.16 \log (f) \quad (107)$$

At Frequency range $1.5 - 2.0$ GHz

$$PL = (44.9 - 6.55 \log (h_{te})) \log (d) + 14.78$$
$$+5.83 \log (h_{te}) + 34.97 \log (f) \quad (108)$$

At Frequency range $2.0 - 6.0$ GHz

$$PL = (44.9 - 6.55 \log (h_{te})) \log (d) + 18.38$$
$$+5.83 \log (h_{te}) + 23 \log (f) \quad (109)$$

where σ_{SF} is 4, applicability range of $10m < d < 2km$, h_{te} is 10m and h_{re} is 1.5m

For the WINNER+ SMa (LoS):

$$PL_1 = 23.8 log (d) + 27.2 + 20.0 \log (f) \quad (110)$$

$$PL_2 = 40.0 \log (d) + 9.0 - 16.2 \log (h_{te})$$
$$- 16.2 \log (h_{re}) + 3.8 \log f \quad (111)$$

where the applicability range and are

$$\begin{cases} PL_1, & 30m < d < d_{BP}, \sigma_{SF} \text{ is } 4 \\ PL_2, & d_{BP} \leq d \leq 5km, \sigma_{SF} \text{ is } 6, \end{cases}$$

h_{te} is 25m, and h_{re}, is 1.5m.

For the WINNER+ SMa (NLoS):
At Frequency range $0.45 - 1.5$ GHz

$$PL = (44.9 - 6.55 \log (h_{te})) \log (d) + 13.33$$
$$+5.83 \log (h_{te}) + 26.16 \log (f) \quad (112)$$

At Frequency range $1.5 - 2.0$ GHz

$$PL = (44.9 - 6.55 \log (h_{te})) \log (d) + 11.78$$
$$+5.83 \log (h_{te}) + 34.97 \log (f) \quad (113)$$

At Frequency range $2.0 - 6.0$ GHz

$$PL = (44.9 - 6.55 \log (h_{te})) \log (d) + 15.38$$
$$+5.83 \log (h_{te}) + 23 \log (f) \quad (114)$$

where σ_{SF} is 8, applicability range of $50m < d < 5km$, h_{te} is 25m and h_{re} is 1.5m

For the WINNER+ UMa (LoS):

$$PL_1 = 26.0 log(d) + 25.0 + 20.0 \log(f) \qquad (115)$$

$$PL_2 = 40.0 \log(d) + 9.27 - 14.0 \log(h'_{te}) \\ - 14.0 \log(h'_{re}) + 6.0 \log f \qquad (116)$$

where the applicability range and are

$$\begin{cases} PL_1, & 10m < d < d'_{BP}, \sigma_{SF} \text{ is } 4 \\ PL_2, & d'_{BP} \leq d \leq 5km, \sigma_{SF} \text{ is } 6, \end{cases}$$

h_{te} is 25m and, h_{re}, is 1.5m.

For the WINNER+ UMa (NLoS):
At Frequency range $0.45 - 1.5$ GHz

$$PL = (44.9 - 6.55 \log(h_{te})) \log(d) + 16.33 \\ + 5.83 \log(h_{te}) + 26.16 \log f \qquad (117)$$

At Frequency range $1.5 - 2.0$ GHz

$$PL = (44.9 - 6.55 \log(h_{te})) \log(d) + 14.78 \\ + 5.83 \log(h_{te}) + 34.97 \log(f) \qquad (118)$$

At Frequency range $2.0 - 6.0$ GHz

$$PL = (44.9 - 6.55 \log(h_{te})) \log(d) + 18.38 \\ + 5.83 \log(h_{te}) + 23 \log(f) \qquad (119)$$

where σ_{SF} is 8, applicability range of $10m < d < 5km$, h_{te} is 25m, and h_{re}, is 1.5m.

S. CLOSE-IN FREE SPACE REFERENCE DISTANCE (CI) PATH LOSS MODELS

The CI path loss models had been used for the estimation of PL in various scenarios and environments for so many years [90], [101], [120]. It is a generic all-frequency model useful in describing the large-scale propagation PL. Amazingly, it has been proven to be useful in modelling the PL of a vast range of mmWave frequencies with good and robust accuracy [121]–[123]. The model has a 1m free space reference distance and very useful in modelling PL for UMa, UMi, InH, and RMa scenarios [124].

The parameter of the attenuation is estimated by the PL model as a function of carrier frequency and distance separation, which is known as fading behaviour [27]. Equation (120) expresses the CI path loss model:

$$PL^{CI}(f, d)[dB] = FSPL(f, d_0) + 10n log_{10}\left(\frac{d}{d_0}\right) + X\sigma^{CI} \qquad (120)$$

where $PL^{CI}(f, d)$ PL at discrete frequencies and transmitter to receiver separation distance, n is PLE (illustrate PL increases rate against distance). $FSPL(f, d_0)$ PL in dB at a close-in (CI) distance, d_0 is 1 m, $X\sigma^{CI}$ is the modelling of the shadow fading (SF) as a zero-mean Gaussian-distributed random variable, σ symbolizes the standard deviation (shadowing effect). The Minimum Mean Square Error (MMSE) method is used for the derivation of PLE and minimum

standard deviation [125]. Since d_0 is 1m as the reference point, FSPL becomes (121):

$$FSPL(f, 1m) = 20log_{10}\left(\frac{4\pi f}{c}\right) \\ = 32.4 + 20log_{10}(f)[dB] \qquad (121)$$

T. FLOATING-INTERCEPT (FI) MODEL

The FI path loss model [105], is also a single frequency PL model, which is applicable in WINNER II [118] and 3GPP standards [101]. The FI path loss model relies on the floating-intercept (α) and the line slope (β) to attain the best least error fit of the accumulated PLs. FI is described by (122):

$$PL^{FI}(d) = \alpha + 10\beta log_{10}(d) + X_\sigma^{FI} \qquad (122)$$

where X_σ^{FI} is a model of the shadow fading as a zero-mean Gaussian-distributed random variable with a standard deviation of σ^{FI}. Just like the CI model, solving for α *and* β is required to achieve σ^{FI}, for the MMSE is used as a best-fit.

U. ALPHA-BETA-GAMMA (ABG) MODEL

ABG model [105] is a multifrequency (three-parameters) PL model developed for the measurement of range of frequency bands. It is a common all frequency models that define large-scale propagation PL [122]. The model comprises of a frequency and distance-dependent terms for the description of PL at different frequencies. ABG can be used for a single frequency modelling where the model is reverted to the existing 3GPP floating-intercept (AB) model with three parameters with γ set to 0 or 2 [118], [121]. The parameter values of α, β, γ and σ are attained from the measurement data using closed-form solution. The ABG model references are 1m for distance and 1 GHz for frequency. Equation (123) illustrates the ABG model:

$$PL^{ABG}(f, d) = 10\alpha log_{10}\left(\frac{d}{d_0}\right) + \beta + 10\gamma log_{10}\left(\frac{f}{f_0}\right) \\ + X_\sigma^{ABG} \\ where\ d \geq 1m\ and\ f \geq 1GHz \qquad (123)$$

where α and γ are constant coefficients indicating the effect of frequency and distance on PL, β is denoted as an optimized offset value for PL, f is the carrier frequency and X_σ^{ABG} is a Gaussian random variable with a standard deviation of σ^{ABG}. The ABG model is resolved by the MMSE method to reduce σ by simultaneously calculating for α, β, and γ [125].

V. CI MODEL WITH A FREQUENCY-WEIGHTED PATH LOSS EXPONENT (CIF)

The CIF uses the same motivated FSPL anchor at 1m just like the CI model, it was developed for multifrequency PL modelling that takes frequency dependency of the PL across a variety of frequencies [126], [103]. Equation (124) illustrates

the CIF model:

$$PL^{CIF}(f,d) = FSPL(f,d_0) + 10n$$
$$\times \left(1 + b\left(\frac{f-f_0}{f_0}\right)\right)\log(d) + X_\sigma^{CIF} \quad (124)$$

where n is the distance dependence of PL (similar to the CI model PLE), while b is a model parameter that notes the PL linear frequency dependence of the model and f_0, is a reference frequency (fixed) that attends as the center of the PLE linear frequency dependency [35].

W. NYUSIM

NYUSIM [127] was developed based on measurement campaigns at multiple mmWave frequencies ranging from 28 GHz to 73 GHz. The measurement was carried out at different outdoor environment and scenarios such as UMi, UMa and RMa [97], [101], [103], [121], [128]–[131]. The model is applicable for frequency ranges from 0.5 - 100 GHz and 0 – 800 MHz RF bandwidths [127].

The CI path loss model with a *1 m* reference distance was modified by adding an attenuation term, which is due to different atmospheric conditions of the environments. The PL is given in (125):

$$PL^{NYU}(f,d) = FSPL(f,1m) + 10n\log_{10}(d)$$
$$+ AT + X\sigma^{CI} \quad (125)$$
$$AT[dB] = \alpha[dB/m] * d[m] \quad (125a)$$

where $d \geq 1m$, AT is the atmospheric attenuation, α is the frequency (1 GHz to 100 GHz) attenuation factor given in *dB*/m, such as the collective attenuation effects of water vapour, dry air, rain, oxygen and haze [132].

X. LONGLEY-RICE MODEL

The model was developed in 1967, where a computer-based program was used to predict the median propagation loss for irregular terrains [133], [134]. It is also referred to as the Irregular Terrain Model (ITM) [135]. The model has two parts: predictions across an area and the point-to-point link prediction. The model can either use a detailed terrain profile of the actual paths or a profile representative of a given median terrain characteristic. The input parameters include the BS and MS antenna heights (variable range of 0.5 to 3000 m), carrier frequency (20 MHz to 40 GHz), polarization, distance (1 to 2000 km), surface refractivity (250 to 400 N) and a terrain profile of the transmission path, ground constant, climate [80], [136]. Note that surface refractivity determines the effective earth radius, which in turn becomes the tropospheric scatter variable [136].

These regions are delineated by the model from the terrain data and the location of the antennas. The model can easily be customized for a broader range of applications because of its ability to input various parameters. A few of the developed excellent freeware programs that use the model are Radio Mobile, SPLAT!, QRadioPredict, Pathloss 5, Probe, Tower-Coverage.com, and Nautel.

1) DETERMINISTIC MODELS (THEORETICAL MODELS)

The model is based on the fundamental principles of EM wave propagation. It employs the laws governing the EM wave propagation to determine the strength of the signal received at any specific scene using reflection and diffraction laws to estimate the signal strength and usually require the 3D map of the proposed propagation area [137]. The model applies to various scenarios without the accuracy been altered. Unfortunately, the process is quite complicated and lacks computational efficiency [138]. Some of the known and widely used deterministic models for the prediction of network coverage area are discussed.

a: WALFISCH-BERTONI (WB) MODEL

The WB Model considered the multiscreen diffraction attenuation of signals due to the rooftops as well as the buildings to predict the average PL at the street level. The PL model is made up of three factors which are: 1) the free space PL, 2) the reduction $Q(\alpha)$ of the rooftop fields due to settling, 3) and the diffraction effect of the rooftop fields [57]. The WB model assumed a uniformed building height in the development of the model [59]. The model is suitable for predicting PL for frequency in the range of 800 MHz to 2 GHz. Equation (126) illustrates the model with the required correction factors ideal for the Urban environment.

$$PL_{WB} = 89.5 + A + 38\log(d) - 18\log(h_{te} - h_b)$$
$$+ 21\log(f) \quad (126)$$

And A is given in (126a)

$$A = 5\log\left[\left(\frac{b}{2}\right)^2 + (h_b - h_{re})^2\right] - 9\log(b)$$
$$+ 20\log\left\{tan^{-1}\left[\frac{2(h_b - h_{re})}{b}\right]\right\} \quad (126a)$$

where h_b is the building height, and b is the center-to-center spacing of the buildings. The model is best suitable for buildings of equal heights, and this is a drawback as the model does not apply to suburban and rural scenarios [139].

b: RAY-TRACING TECHNIQUES

The technique is based on Geometrical Optics, an approximate method used for high-frequency levels estimation [33]. Geometrical Optics assumed the possibility of energy been radiated through small tubes (known as rays, which are equivalent to signal power) [140]. Rays are known to travel in the direction of propagation in straight lines as long as the channel's relative refractive index is constant [33], [141]. This provides the possibility of modelling cellular signals via ray propagation.

The ray-tracing PL models are used for predicting the process of the physical propagation of signals in a given environment. It requires the building of the 3D topographic database as well as the proper models for environment interactions (such as the diffraction, scattering, and reflection of the environments) [142]. Maxwell's equations having an

appropriate boundary are used for determining the multipath propagation. However, due to the computational complexity, the multipath effects are approximated using geometric equations. The method has been useful for the propagation characteristic modelling in small cells (Microcells) [143], [144], large cells [145], medium-sized cells (picocell) [146]. The determination of the dominant ray paths of signal propagation is key to using ray-tracing PL to determine an accurate PL prediction; this also makes the computational process faster [147].

There are two main types of ray-tracing techniques, namely, the image method [148]–[151] and the brute-force ray-tracing method [33]. Other types had been developed, such as a three-dimensional (3D) ray-tracing propagation model [152], a hybrid three-dimensional (3-D) ray-tracing algorithm [143]. Two-Ray Model (the received signal power is illustrated in (127)), Dielectric Canyon (Ten-Ray Model), General Ray Tracing (GRT) [153]. Some of the computer programs combine aerial graphics or architectural drawing to achieve the 3D geometric picture of the scenarios, and such programs include Lucent's Wireless Systems Engineering software (WiSE), Wireless Valley's Site Planner and Marconi's Planet EV [2].

$$P_r\,(dBm) = P_t\,(dBm) + 10\log\,(G_l)$$
$$+ 20\log\,(h_{re}h_{te}) - 40\log\,(d) \qquad (127)$$

c: FINITE-DIFFERENCE TIME-DOMAIN (FDTD) MODEL

FDTD [154] is an alternative technique to estimate the radio wave propagation by solving the Maxwell equations on a discrete spatial and temporal grid. The model accommodated the disadvantage of the Ray-tracing by accounting for all reflections and diffractions in its formulation [155]. The FDTD model is known for its higher accuracy, which can also concurrently deliver a comprehensive solution for all the points in the map, therefore, providing accurate and complete signal coverage over a given area [33]. Unfortunately, the model is computationally intensive, which require a high time-consuming algorithm [156]. This model is suitable for both indoor and outdoor scenarios [157]. Over the years, researches have been made to reduce the computational time and, in general, improve the model. More details can be found in [158]–[163].

d: ARTIFICIAL NEURAL NETWORKS (ANN)

ANN is an artificial intelligence technique as well as an information processing system made up of interconnected simple processing elements, which is designed to compute a parallel distributed process to a specific task such as function approximation, prediction, optimization, control, among others [164]. The ANN model [165] was developed using the principles of feedforward neural networks (FNN) [166]. This model displayed better performance in solving issues associated with mild nonlinearity as a result of noisy data by using the FNN with sigmoidal activation functions. Unlike the other deterministic models, ANN has a fast process of

predicting the signal strength due to the intrinsic parallelism, which allows for a quick appraisal of the solutions [165].

ANN solves a given problem by determining the coefficients between the inputs and the outputs, that is, it makes the connections between the two layers (input and output) through a learning system. Various researches have shown the successful performance of the PL prediction in rural [167], suburban [168], urban [169] as well as indoor environments. Data collected for the environments are usually used for the training of the model to predict the PL. Therefore, measurement data from various environments used for the training process would lead to a more accurate model. The performance is also determined by the chosen input parameters [170]. Further discussions on other artificial intelligent models or machine learning methods are available at [171].

V. COMPARATIVE ANALYSIS OF PROPAGATION MODELS

This section provides a summary study of the different path loss models used for predicting the network coverage area, and the models are classified based on factors such as frequency range, type of terrain, mobile generation, as shown in Table 6.

Cellular communication systems operate on different frequency bands ranging from 450 MHz to 40 GHz. Each of the mobile communication generations is assigned frequency band to operate, the 1G uses frequency bands of 800 MHz to 900 MHz, 2G uses more and various frequency bands which are 850MHz, 900 MHz, 1800 MHz and 1900 MHz (depending on the country of deployed). The 3G frequency bands are 800 MHz, 850 MHz, 900 MHz, 1700 MHz 1900 MHz, and 2100 MHz (also depends on the country of deployment).

The 4G has the same frequency band just like the 3G but with the addition of 2300 MHz, 2500 MHz and 2600 MHz. On the other hand, the 5G will be using Frequency range 1 (FR1). This includes all the 4G frequency range (450 MHz to 6 GHz) and Frequency range 2 (FR2), which is from 24.25 GHz to 52.6 GHz.

The PL experienced by signals as it propagates from one point (transmitter) to another point (receiver) over distance are compared for the different PL models. The comparison is grouped into three as shown in Table 7, comprising of PL models, the carrier frequency as well the BS and MS heights.

The PL models are plotted against distance, the frequency range in which the models were developed were considered for the grouping. Figure 4 compared the Okumura Hata, Ericsson 9999, COST231, Egli, and the ECC-33 model at the stated frequency. Figure 5 compared the 3GPP-SCM, WINNER I, TR 36.873 and ITU-R. These models were designed for the frequency range of 2GHz to 6 GHz. Figure 6 compared the Close-In, ABG and FI models. The models were developed to predict coverage area for the mmWave band, useful for 5G networks.

VI. EMERGING TECHNOLOGY

The development and advancement of the cellular communications network had been on a great increase. Apart from

TABLE 6. Classification of the path loss models.

Citations	Year	Model name	Frequency range	Type of Terrain	Mobile generation
[81], [82]	1957	Egli Model	90 MHz- 1 GHz	Irregular terrain	1G and 2G
[44]	1960	Okumura et al. Model	150 MHz - 1.92 GHz	Urban, Suburban, and Rural	1G and 2G
[135], [172]	1966	FDTD model	Applicable to any frequency	Urban, Suburban, and Rural	All mobile generations
[133], [134]	1967	Longley-rice model	20 MHz to 40 GHz	Irregular terrains	All mobile generations
[46]	1980	Okumura-Hata Model	150 MHz - 1.5 GHz	Urban, Suburban and Open Environment	1G and 2G
[173]	1982	Lee Model	900 MHz frequency	Free space area, Rural, suburban and urban	1G, 2G
[86], [88]	1984	Log-normal Shadowing Model	Applicable to any frequency	Free space area, Urban	All mobile generations
[57], [68]	1988	Walfisch-Bertoni Model	800 MHz to 2 GHz	Urban environments	1G, 2G, and 3G
[150]	1991	Ray-tracing techniques	Applicable to any frequency	Plain earth	All mobile generations
[167]	1992	ANN	All frequency	Urban, Suburban, and Rural	All mobile generation
[69], [70]	1997	Ericsson Model	150 MHz - 2 GHz	Urban, Suburban, and Rural	1G, 2G, and 3G
[90], [101], [120]	1997	CI Path Loss Model	Applicable to any frequency	Urban, Suburban, and Rural	2G, 3G, 4G, and 5G
[51], [139]	1999	COST 231-Hata Model	1.5 GHz - 2 GHz	Urban, Suburban, and Rural (Flat)	1G, 2G, and 3G
[54]	1999	COST 231-WI Model	800 MHz - 2 GHz	Metropolitan center, Urban, Suburban & Rural	1G, 2G, and 3G
[62], [63]	2001	COST 259	800 MHz - 5 GHz	Urban, bad urban, Rural, and hilly terrain	2G, 3G, and 4G
[72], [73],[77]	2001	SUI Model	1.9 GHz -11 GHz	Hilly, Flat environment, Suburban,	3G and 4G
[65]	2003	ECC-33 Model	700 MHz - 3.5 GHz	Medium and large cities, Urban, Suburban, Rural, and open area	1G, 2G, 3G, and 4G
[117]	2005	WINNER I Model	2 and 5 GHz	Urban, Suburban, and Rural	2G and 3G
[108]	2009	ITU–R models	2 GHz - 6GHz 450 MHz to 6 GHz	Urban, Suburban, and Rural	2G, 3G, and 4G
[118]	2009	WINNER II	2 – 6 GHz	Urban, Suburban, and Rural	2G, 3G, and 4G
[119]	2010	WINNER+	450 MHz to 6 GHz	Urban, Suburban, and Rural	2G, 3G, and 4G
[94]	2011	3GPP SCM	1 GHz to 3 GHz	Urban, Suburban, and Rural	2G, 3G, and 4G
[105], [101], [118]	2013	FI path loss model	mmWave frequency	Urban, Suburban, and Rural	Designed specifically for 5G
[105], [122]	2013	ABG Model	Applicable to any frequency	Urban, Suburban, and Rural	2G, 3G, 4G, and 5G
[115]	2014	MiWEBA	60 GHz frequency band	Open area (University campus), Urban (Street Canyon)	Designed specifically for 5G
[92]	2015	Blocked LoS	500 MHz - 100 GHz	Urban, Suburban, and Rural	2G, 3G, 4G, and 5G
[106], [107]	2015	METIS	450 MHz - 60 GHz	Dense urban, urban, Rural, highway	Designed specifically for 5G
[114]	2015	mmMAGIC	6 GHz - 100 GHz	Urban (Street Canyon), Stadium and Metro station	Designed specifically for 5G
[126], [103]	2015	CIF path loss Model	Applicable to any frequency	Urban, Suburban, and Rural	2G, 3G, 4G, and 5G
[99]	2016	5GCM	6 GHz - 100 GHz	Urban (Street Canyon and Open Square), O2O, O2I	Designed specifically for 5G
[95]	2017	3GPP TR 36.873	2 GHz – 6 GHz	Urban, Suburban, and Rural	4G
[98]	2017	3GPP TR 38.901	500 MHz – 100 GHz	Urban (street canyon open area), Suburban	Designed specifically for 5G
[108]	2017	NYUSIM	500 MHz – 100 GHz	Urban, Rural	Designed for 5G

using the appropriate PL models to improve the quality of signals, other concepts contribute to improving the communication network in general. Over the years, there has been

relentless pursuit to expand and increase the capacity of the cellular networks to support higher data rates. Optimizing the aspect of the communication system has been the focus

TABLE 7. Simulation parameters and specifications.

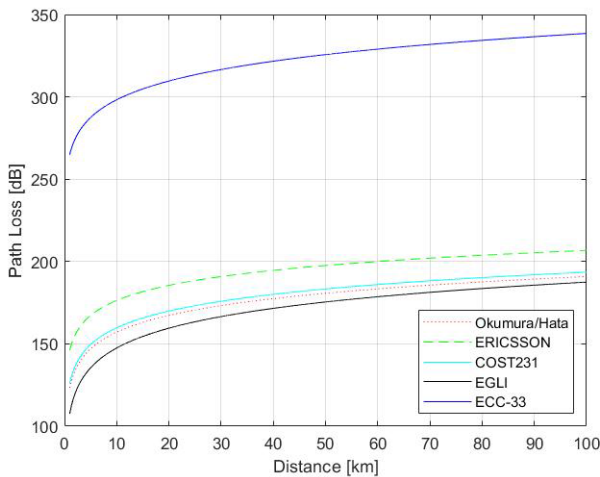| Groups	PL Models	Carrier Frequency	BS/MS antenna height (m)
A	Okumura/Hata, Ericsson, COST231, Egli, ECC-33	900 MHz	50/1.5
B	3GPP-SCM, WINNER I, TR 36.873, ITU-R	2.1 GHz	50/2
C	Close-In, ABG, FI Models	28 GHz	30/2

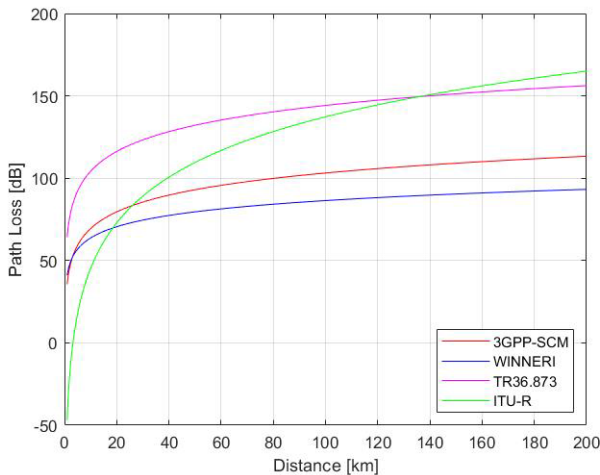**FIGURE 4.** Plot showing path loss Models against the distance of Group A.

FIGURE 5. Plot showing path loss Models against distance of Group B.

FIGURE 6. Plot showing path loss Models against distance of Group C.

thereby given us the partial control of the wireless channel to deliver more satisfactory propagation characteristics. Generally, reflection, mirroring and scattering effects had been treated as uncontrollable phenomena and had been modelled stochastically. However, with the advent of RIS, these effects are rather considered as part of the parameters of the system that could be optimized, this allows overcoming various challenges of wireless communications.

The RIS concept is comparable to the massive MIMO Comparing IRSs with massive MIMO [175] and other related technologies, where improvement of spectral and energy efficiencies was achieved by using large arrays of antennas for 5G networks, Hence, RIS is envisioned to be used for the 6G communication networks. The RIS tunes the propagation environment for the communication which is different from how massive MIMO operates [176], [177].

VII. CONCLUSION

Cell coverage area prediction is a vital and essential task in the planning of any wireless radio access system. In most cases, it may be challenging to estimate or determine how various variables would affect signal propagation. Coverage prediction makes use of various path loss (propagation) models to determine the expected network characteristics, received signal strength, area of coverage, and if the desired QoS has been achieved. Path loss models are usually developed based on the need for wireless networks to attain some goals.

Network coverage prediction has been used for easy deployment of cellular networks over the years. Therefore, detailed knowledge of the appropriate path loss model suitable for the proposed geographical area is needed to determine the coverage quality of any wireless network design. However, to the best of our knowledge, despite the importance of Path loss models, as used for the prediction of wireless network coverage, there does not exist any up to date comprehensive survey in this field. Therefore, the purpose of this paper is to survey the existing techniques and

of designers, the process was initiated with multiplexing techniques such as orthogonal frequency-division multiplexing (OFDM), adaptive coding techniques, beamforming (MIMO), frequency reuse, advanced adaptive modulation and inter-cell coordination techniques [174]. Recently, the initiation of reconfigurable intelligent surfaces (RIS), as well as the advent of smart radio environment concept [173], has given the opportunity to control the ambient environment
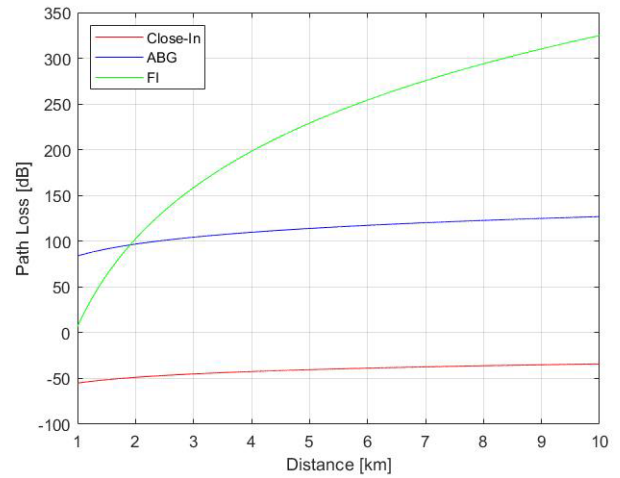
mechanisms which can be addressed in this domain. This work presented a comprehensive and up to date survey of the various network coverage prediction techniques, indicating the various frequency ranges the models were developed for. The various suitable terrains for each of the model and the best suit mobile generation were presented. Likewise, it has provided a comparative analysis to aid the planning and implementation of cellular networks. Other path loss models exist however, this survey only considered propagation models for large-scale fading and outdoor scenarios.

ACKNOWLEDGMENT

REFERENCES

[1] O. O. Erunkulu, E. N. Onwuka, O. Ugweje, and L. A. Ajao, "Prediction of call drops in GSM network using artificial neural network," *Jurnal Teknologi dan Sistem Komputer*, vol. 7, no. 1, p. 38, 2019.

[2] T. S. Rappaport, *Wireless Communications—Principles and Practice*, 2nd ed. Upper Saddle River, NJ, USA: Prentice-Hall, 2001.

[3] A. Ayeni, N. Faruk, O. Lukman, M. Y. Muhammad, and M. I. Gumel, "Comparative assessments of some selected existing radio propagation models: A study of Kano City, Nigeria," *Eur. J. Sci. Res.*, vol. 70, no. 1, pp. 120–127, 2012.

[4] D. Yuan and D. Shen, "Analysis of the Bertoni-Walfisch propagation model for mobile radio," in *Proc. 2nd Int. Conf. Mechanic Autom. Control Eng.*, Jul. 2011, pp. 77–80.

[5] T. Eyceoz, A. Duel-Hallen, and H. Hallen, "Deterministic channel modeling and long range prediction of fast fading mobile radio channels," *IEEE Commun. Lett.*, vol. 2, no. 9, pp. 254–256, Sep. 1998.

[6] A. Duel-Hallen, "Fading channel prediction for mobile radio adaptive transmission systems," *Proc. IEEE*, vol. 95, no. 12, pp. 2299–2313, Dec. 2007.

[7] J. B. Andersen, J. Jensen, S. H. Jensen, and F. Frederiksen, "Prediction of future fading based on past measurements," in *Proc. IEEE Veh. Technol. Conf.*, Sep. 1999, vol. 50, no. 1, pp. 151–155.

[8] T. Ekman, "Prediction of mobile radio channels, modeling and design," Ph.D. dissertation, Dept. Elect. Eng., Signals Syst., Uppsala Univ., Uppsala, Sweden, Oct. 2002.

[9] L. Dong, G. Xu, and H. Ling, "Prediction of fast fading mobile radio channels in wideband communication systems," in *Proc. IEEE GLOBECOM Telecommun. Conf. (GLOBECOM)*, Nov. 2001, vol. 6, no. 1, pp. 3287–3291.

[10] N. Palleit and T. Weber, "Channel prediction in multiple antenna systems," in *Proc. Int. ITG Workshop Smart Antennas (WSA)*, Mar. 2012, pp. 1–7.

[11] K. Yamaguchi, H. P. Bui, Y. Ogawa, T. Nishimura, and T. Ohgane, "Channel prediction techniques for a multi-user MIMO system in time-varying environments," *IEICE Trans. Commun.*, vol. E97.B, no. 12, pp. 2747–2755, 2014.

[12] Z. Mokhtari, M. Sabbaghian, and R. Dinis, "A survey on massive MIMO systems in presence of channel and hardware impairments," *Sensors*, vol. 19, no. 1, p. 164, Jan. 2019.

[13] X. Chaochen, T. Xiaoheng, T. Balginbek, Q. Qian, and Z. Xiaoliang, "Research of resource allocation technology based on MIMO ultra density heterogeneous network for 5G," in *Proc. Comput. Sci. 8th Int. Congr. Inf. Commun. Technol.*, vol. 131, 2018, pp. 1039–1047.

[14] P. Almers, E. Bonek, A. Burr, N. Czink, M. Debbah, V. Degli-Esposti, H. Hofstetter, P. Kyösti, D. Laurenson, G. Matz, A. F. Molisch, C. Oestges, and H. Özcelik, "Survey of channel and radio propagation models for wireless MIMO systems," *EURASIP J. Wireless Commun. Netw.*, vol. 2007, no. 1, Dec. 2007, Art. no. 019070.

[15] S. A. Busari, K. M. S. Huq, S. Mumtaz, L. Dai, and J. Rodriguez, "Millimeter-wave massive MIMO communication for future wireless systems: A survey," *IEEE Commun. Surveys Tuts.*, vol. 20, no. 2, pp. 836–869, 2nd Quart., 2018.

[16] W. Khawaja, I. Guvenc, D. W. Matolak, U.-C. Fiebig, and N. Schneckenburger, "A survey of air-to-ground propagation channel modeling for unmanned aerial vehicles," *IEEE Commun. Surveys Tuts.*, vol. 21, no. 3, pp. 2361–2391, 3rd Quart., 2019.

[17] W. Khawaja, I. Guvenc, and D. Matolak, "UWB channel sounding and modeling for UAV air-to-ground propagation channels," in *Proc. IEEE Global Commun. Conf. (GLOBECOM)*, Dec. 2016, pp. 1–7.

[18] A. Akinbolati, M. O. Ajewole, A. T. Adediji, and J. S. Ojo, "Propagation curves and coverage areas of digital terrestrial television base stations in the tropical zone," *Heliyon*, vol. 6, no. 3, pp. 1–16, 2020.

[19] S. Kasampalis, P. I. Lazaridis, Z. D. Zaharis, A. Bizopoulos, S. Zettas, and J. Cosmas, "Comparison of Longley-Rice, ITU-R P.1546 and Hata-Davidson propagation models for DVB-T coverage prediction," in *Proc. IEEE Int. Symp. Broadband Multimedia Syst. Broadcast.*, Jun. 2014, p. 1546.

[20] S. Kasampalis, P. I. Lazaridis, Z. D. Zaharis, A. Bizopoulos, S. Zettas, and J. Cosmas, "Comparison of ITM and ITWOM propagation models for DVB-T coverage prediction," in *Proc. IEEE Int. Symp. Broadband Multimedia Syst. Broadcast. (BMSB)*, Jun. 2013, pp. 1–4.

[21] Y. Wang, Y. Si, and H. Leung, "A novel inversion method for outdoor coverage prediction in wireless cellular network," *IEEE Trans. Veh. Technol.*, vol. 59, no. 1, pp. 36–47, Jan. 2010.

[22] N. C. Goncalves and L. M. Correia, "A propagation model for urban microcellular systems at the UHF band," *IEEE Trans. Veh. Technol.*, vol. 49, no. 4, pp. 1294–1302, Jul. 2000.

[23] C. Takahashi, Z. Yun, M. Iskander, G. Poilasne, V. Pathak, and J. Fabrega, "Propagation-prediction and site-planning software for wireless communication systems," *IEEE Antennas Propag. Mag.*, vol. 49, no. 2, pp. 52–60, Apr. 2007.

[24] E. Amaldi, A. Capone, and F. Malucelli, "Radio planning and coverage optimization of 3G cellular networks," *Wireless Netw.*, vol. 14, no. 4, pp. 435–447, Aug. 2008.

[25] E. Ekiz and R. Sokullu, "Comparison of path loss prediction models and field measurements for cellular networks in Turkey," in *Proc. Int. Conf. Sel. Topics Mobile Wireless Netw. (iCOST)*, Oct. 2011, pp. 48–53.

[26] *ITU Radiocommunication Sector*. Accessed: May 5, 2020. [Online]. Available: https://www.itu.int/en/ITU-R/Pages/default.aspx

[27] M. B. Majed, T. A. Rahman, O. A. Aziz, M. N. Hindia, and E. Hanafi, "Channel characterization and path loss modeling in indoor environment at 4.5, 28, and 38 GHz for 5G cellular networks," *Int. J. Antennas Propag.*, vol. 2018, pp. 1–14, Sep. 2018.

[28] A. Neskovic, N. Neskovic, and G. Paunovic, "Modern approaches in modeling of mobile radio systems propagation environment," *IEEE Commun. Surveys Tuts.*, vol. 3, no. 3, pp. 2–12, 3rd Quart., 2000.

[29] A. S. Abdulrasool, J. S. Aziz, and S. J. Abou-Loukh, "Calculation algorithm for diffraction losses of multiple obstacles based on Epstein–Peterson approach," *Int. J. Antennas Propag.*, vol. 2017, pp. 1–9, Oct. 2017.

[30] T. L. Singal, *Wireless Communications*, 1st ed. New Delhi, India: McGraw-Hill, 2010, p. 43.

[31] V. S. Anusha, G. K. Nithya, and S. N. Rao, "A comprehensive survey of electromagnetic propagation models," in *Proc. Int. Conf. Commun. Signal Process. (ICCSP)*, Apr. 2017, pp. 1457–1462.

[32] C. Phillips, D. Sicker, and D. Grunwald, "A survey of wireless path loss prediction and coverage mapping methods," *IEEE Commun. Surveys Tuts.*, vol. 15, no. 1, pp. 255–270, 1st Quart., 2013.

[33] T. K. Sarkar, Z. Ji, K. Kim, A. Medouri, and M. Salazar-Palma, "A survey of various propagation models for mobile communication," *IEEE Antennas Propag. Mag.*, vol. 45, no. 3, pp. 51–82, Jun. 2003.

[34] J. Milanović, S. Rimac-Drlje, and I. Majerski, "Radio wave propagation mechanisms and empirical models for fixed wireless access systems," *Tehnički vjesnik*, vol. 17, no. 1, pp. 43–52, 2010.

[35] S. Sun, G. R. MacCartney, and T. S. Rappaport, "Millimeter-wave distance-dependent large-scale propagation measurements and path loss models for outdoor and indoor 5G systems," in *Proc. 10th Eur. Conf. Antennas Propag. (EuCAP)*, Apr. 2016, pp. 1–5.

[36] S. Yelen, S. Selim Seker, and F. C. Kunter, "Radio propagation path loss prediction of UMTS for an urban area," in *Proc. Dig. 14th Biennial IEEE Conf. Electromagn. Field Comput.*, May 2010, pp. 902–905.

[37] M. Olsson, C. Cavdar, P. Frenger, S. Tombaz, D. Sabella, and R. Jantti, "5GrEEn: Towards green 5G mobile networks," in *Proc. IEEE 9th Int. Conf. Wireless Mobile Comput., Netw. Commun. (WiMob)*, Oct. 2013, pp. 212–216.

[38] O. C. I. Omeje, A. Chukwuneke, and V. N. Okorogu, "Multipath interference reduction in wireless radio systems using two-branch selection diversity," *Int. J. Adv. Sci. Res. Eng.*, vol. 3, no. 8, pp. 21–29, 2017.

[39] M. U. Sheikh, J. Säe, and J. Lempiäinen, "Multipath propagation analysis of 5G systems at higher frequencies in courtyard (small cell) environment," in *Proc. IEEE 5G World Forum, 5GWF Conf.*, Jul. 2018, pp. 239–243.

[40] J. J. Park, J. Lee, K. W. Kim, M. D. Kim, and K. C. Lee, "Multipath propagation characteristics for 5G vehicular communications based on 28 GHz expressway measurements," in *Proc. 13th Eur. Conf. Antennas Propag. (EuCAP)*, 2019, pp. 1–5.

[41] C. U. Bas, R. Wang, S. Sangodoyin, S. Hur, K. Whang, J. Park, J. Zhang, and A. F. Molisch, "28 GHz microcell measurement campaign for residential environment," in *Proc. IEEE Global Commun. Conf. (GLOBECOM)*, Dec. 2017, pp. 1–6.

[42] T. A. Benmus, R. Abboud, and M. K. Shater, "Neural network approach to model the propagation path loss for great Tripoli area at 900, 1800 and 2100 MHz bands," *Int. J. Sci. Tech. Autom. Control Eng.*, vol. 10, no. 2, pp. 2121–2126, 2016.

[43] Z. Naseem, I. Nausheen, and Z. Mirza, "Propagation models for wireless communication system," *Int. Res. J. Eng. Technol.*, vol. 5, no. 1, pp. 1–6, 2018.

[44] Y. Okumura, E. Ohmori, T. Kawano, and K. Fukuda, "Field strength and its variability in VHF and UHF land mobile radio service," *Rev. Elect. Commun. Lab.*, vol. 16, nos. 9–10, pp. 825–873, 1968.

[45] M. F. Iskander and Z. Yun, "Propagation prediction models for wireless communication systems," *IEEE Trans. Microw. Theory Techn.*, vol. 50, no. 3, pp. 662–673, Mar. 2002.

[46] M. Hata, "Empirical formula for propagation loss in land mobile radio services," *IEEE Trans. Veh. Technol.*, vol. VT-29, no. 3, pp. 317–325, Aug. 1980.

[47] S. Bolli and M. Z. A. Khan, "A novel LMMSE based optimized Perez-Vega Zamanillo propagation path loss model in UHF/VHF bands for India," *Prog. Electromagn. Res. B*, vol. 63, pp. 17–33, Apr. 2015.

[48] M. Farhoud, A. El-Keyi, and A. Sultan, "Empirical correction of the Okumura-Hata model for the 900 MHz band in egypt," in *Proc. 3rd Int. Conf. Commun. Inf. Technol. (ICCIT)*, Jun. 2013, pp. 386–390.

[49] *Digital Land Mobile Radio Communications*, Luxembourg City, Luxembourg, COST 207 Report, 1989.

[50] D. Laurenson, D. G. M. Cruickshank, and G. J. R. Poveq, "A computationally efficient multipath channel simulator for the cost 207 models," in *Proc. IEE Colloq. Comput. Modeling Commun. Syst.*, 1994, pp. 8-1–8-6.

[51] P. E. Mogensen and J. Wigard, "COST action 231, digital mobile radio towards future generation systems: Final report," EU Publications, Brussels, Belgium, Tech. Rep., 1999.

[52] N. Rakesh and D. Nalineswari, "Comprehensive performance analysis of path loss models on GSM 940 MHz and IEEE 802.16 WIMAX frequency 3.5 GHz on different terrains," in *Proc. Int. Conf. Comput. Commun. Informat. (ICCCI)*, Jan. 2015, pp. 1–7.

[53] Z. K. Adeyemo, A. O. Akande, and A. O. Fawole, "Investigation of some existing prediction models and development of a modified model for UMTS signal in Owerri, Nigeria," *Int. J. Commun. Antenna Propag.*, vol. 7, no. 4, pp. 290–297, 2017.

[54] M. S. Smith and J. E. J. Dalley, "A new methodology for deriving path loss models from cellular drive test data," in *Proc. Millennium Conf. Antennas Propag. (AP)*, Davos, Switzerland, vol. 2, Apr. 2000.

[55] X. Chu, D. Lopez-Perez, Y. Yang, and F. Gunnarsson, *Heterogeneous Cellular Networks: Theory, Simulation and Deployment*, 1st ed. Cambridge, U.K.: Cambridge Univ. Press, 2020.

[56] A. Zreikat and M. Dordevic, "Performance analysis of path loss prediction models in wireless mobile networks in different propagation environments," in *Proc. 3rd World Congr. Electr. Eng. Comput. Syst. Sci.*, Jun. 2017, pp. 1–11.

[57] J. Walfisch and H. L. Bertoni, "A theoretical model of UHF propagation in urban environments," *IEEE Trans. Antennas Propag.*, vol. 36, no. 12, pp. 1788–1796, Dec. 1988.

[58] Y. A. Alqudah, "On the performance of cost 231 Walfisch Ikegami model in deployed 3.5 GHz network," in *Proc. Int. Conf. Technol. Adv. Electr., Electron. Comput. Eng. (TAEECE)*, May 2013, pp. 524–527.

[59] A. Bhuvaneshwari, R. Hemalatha, and T. Satyasavithri, "Semi deterministic hybrid model for path loss prediction improvement," in *Proc. 2nd Int. Conf. Intell. Comput., Commun. Converg. Comput. Sci.*, vol. 92, 2016, pp. 336–344.

[60] L. Juan-Llacer, L. Ramos, and N. Cardona, "Application of some theoretical models for coverage prediction in macrocell urban environments," *IEEE Trans. Veh. Technol.*, vol. 48, no. 5, pp. 1463–1468, Sep. 1999.

[61] A. Tajvidy and A. Ghorbani, "A new uniform theory-of-diffraction-based model for the multiple building diffraction of spherical waves in microcell environments," *Electromagnetics*, vol. 28, no. 5, pp. 375–387, Jun. 2008.

[62] L. M. Correia, *Wireless Flexible Personalized Communications–COST 259: European Co-operation in Mobile Radio Research*, 1st ed. New York, NY, USA: Wiley, 2001.

[63] H. Asplund, A. A. Glazunov, A. F. Molisch, K. I. Pedersen, and M. Steinbauer, "The COST 259 directional channel model—Part II: Macrocells," *IEEE Trans. Wireless Commun.*, vol. 5, no. 12, pp. 3434–3449, Dec. 2006.

[64] F. Ikegami, S. Yoshida, T. Takeuchi, and M. Umehira, "Propagation factors controlling mean field strength on urban streets," *IEEE Trans. Antennas Propag.*, vol. 32, no. 8, pp. 822–829, Aug. 1984.

[65] ECC, "The analysis of the coexistence of FWA cells in the 3.4–3.8 GHz band," in *Proc. Eur. Conf. Postal Telecommun. Admin. (ECC 33)*, 2003.

[66] V. S. Abhayawardhana, I. J. Wassellt, D. Crosby, M. P. Sellars, and M. G. Brown, "Comparison of empirical propagation path loss models for fixed wireless access systems," in *Proc. IEEE 61st Veh. Technol. Conf.*, May 2005, vol. 61, no. 1, pp. 73–77.

[67] M. Kumar, V. Kumar, and S. Malik, "Performance and analysis of propagation models for predicting RSS for efficient handover," *Int. J. Adv. Sci. Tech. Res.*, vol. 1, no. 2, pp. 61–70, 2012.

[68] W. Lambrechts and S. Sinha, "Terrestrial and millimeter-wave mobile backhaul: A last mile solution," in *Last Mile Internet Access for Emerging Economies*. Cham, Switzerland: Springer, 2019, pp. 143–183.

[69] Ericsson, "Basic concepts of WCDMA radio access network," Ericsson Radio Syst. AB, Stockholm, Sweden, White Paper, 2001.

[70] C. Chevallier, C. Brunner, A. Garavaglia, K. P. Murray, and K. R. Baker, "WCDMA deployment handbook," in *Planning and Optimization Aspects*. Hoboken, NJ, USA: Wiley, 2006.

[71] S. O. Ajose and A. L. Imoize, "Propagation measurements and modelling at 1800 MHz in Lagos Nigeria," *Int. J. Wireless Mobile Comput.*, vol. 6, no. 2, pp. 165–174, 2013.

[72] V. Erceg, K. V. S. Hari, M. S. Smith, D. S. Baum, K. P. Sheikh, C. Tappenden, J. M. Costa, C. Bushue, A. Sarajedini, R. Schwartz, D. Branlund, T. Kaitz, and D. Trinkwon, *Channel Models for Fixed Wireless Applications*, Standard IEEE 802.16.3c-01/29r4, IEEE P802.16, Broadband Wireless Working Group, 2001, pp. 1–36.

[73] V. Erceg, L. J. Greenstein, S. Y. Tjandra, S. R. Parkoff, A. Gupta, B. Kulic, A. A. Julius, and R. Bianchi, "An empirically based path loss model for wireless channels in suburban environments," *IEEE J. Sel. Areas Commun.*, vol. 17, no. 7, pp. 1205–1211, Jul. 1999.

[74] N. Shabbir, M. T. Sadiq, H. Kashif, and R. Ullah, "Comparison of radio propagation models for long term evolution (LTE) network," *Int. J. Next-Gener. Netw.*, vol. 3, no. 3, pp. 27–41, 2011.

[75] Y. A. Alqudah, "Path loss modeling based on field measurements using deployed 3.5 GHz WiMAX network," *Wireless Pers. Commun.*, vol. 69, no. 2, pp. 793–803, 2013.

[76] J. Milanovic, S. Rimac-Drlje, and K. Bejuk, "Comparison of propagation models accuracy for WiMAX on 3.5 GHz," in *Proc. 14th IEEE Int. Conf. Electron., Circuits Syst.*, Dec. 2007, pp. 111–114.

[77] G. Senarath *et al.* (2007). *Multi-Hop Relay System Evaluation Methodology (Channel Model and Performance Metric)*. [Online]. Available: http://ieee802.org/16/relay/docs/80216j-06_013r3.pdf

[78] D. Dobrilovic, M. Malic, D. Malic, and S. Sladojevic, "Analyses and optimization of lee propagation model for LoRa 868 MHz network deployments in urban areas," *J. Eng. Manage. Competitiveness*, vol. 7, no. 1, pp. 55–62, 2017.

[79] S. Karthika, "Path loss study of lee propagation model," *Int. J. Eng. Tech.*, vol. 3, no. 5, pp. 114–117, 2017.

[80] J. D. Parsons, *The Mobile Radio Propagation Channel*, 2nd ed. Hoboken, NJ, USA: Wiley, 2000, pp. 52–70.

[81] J. Egli, "Radio propagation above 40 MC over irregular terrain," *Proc. IRE*, vol. 45, no. 10, pp. 1383–1391, 1957.

[82] J. S. Seybold, *Introduction to RF Propagation*, 1st ed. Hoboken, NJ, USA: Wiley, 2005.

[83] J. Chebil, A. K. Lwas, M. R. Islam, and A.-H. Zyoud, "Comparison of empirical propagation path loss models for mobile communications in the suburban area of Kuala Lumpur," in *Proc. 4th Int. Conf. Mechatronics (ICOM)*, May 2011, pp. 1–5.

[84] N. T. Surajudeen-Bakinde, N. Faruk, S. I. Popoola, M. A. Salman, A. A. Oloyede, L. A. Olawoyin, and C. T. Calafate, "Path loss predictions for multi-transmitter radio propagation in VHF bands using adaptive neuro-fuzzy inference system," *Eng. Sci. Technol., Int. J.*, vol. 21, no. 4, pp. 679–691, Aug. 2018.

[85] M. Garah, L. Djouane, H. Oudira, and N. Hamdiken, "Path loss models optimization for mobile communication in different areas," *Indones. J. Electr. Eng. Comput. Sci.*, vol. 3, no. 1, pp. 126–135, 2016.

[86] D. C. Cox, R. R. Murray, and A. W. Norris, "800-MHz attenuation measured in and around suburban houses," *AT&T Bell Laboratories Tech. J.*, vol. 63, no. 6, pp. 921–954, Jul. 1984.

[87] R. Desimone, B. M. Brito, and J. Baston, "Model of indoor signal propagation using log-normal shadowing," in *Proc. Long Island Syst., Appl. Technol.*, May 2015, pp. 1–4.

[88] R. Bernhardt, "Macroscopic diversity in frequency reuse radio systems," *IEEE J. Sel. Areas Commun.*, vol. 5, no. 5, pp. 862–870, Jun. 1987.

[89] M. Viswanathan, "Wireless channel models," in *Wireless Communication Systems in MATLAB*, 2nd ed. Uttar Pradesh, India: Independently Published, 2018.

[90] T. S. Rappaport, *Wireless Communications Principles and Practice*, 2nd ed. Upper Saddle River, NJ, USA: Prentice-Hall, 1996.

[91] D. Wang, L. Song, X. Kong, and Z. Zhang, "Near-ground path loss measurements and modeling for wireless sensor networks at 2.4 GHz," *Int. J. Distrib. Sens. Netw.*, vol. 8, no. 8, pp. 1–10, 2012.

[92] D. Chizhik, R. A. Valenzuela, and S. Venkatesan, "Physical limits on beam switching performance of LOS mmwave links," Bell Labs, Providence, NY, USA, Tech. Rep. ITD-15-55823C, 2015.

[93] J. Du, E. Onaran, D. Chizhik, S. Venkatesan, and R. A. Valenzuela, "Gbps user rates using mmwave relayed backhaul with high-gain antennas," *IEEE J. Sel. Areas Commun.*, vol. 35, no. 6, pp. 1363–1372, Jun. 2017.

[94] *Universal Mobile Telecommunications System (UMTS); Spatial Channel Model for Multiple Input Multiple Output (MIMO) Simulations*, document 3GPP TR 25.996, V11.0.0, 2011, pp. 16–18.

[95] *Study on 3D channel model for LTE*, document 3GPP TR 36.873, 3rd Generation Partnership Project V12.7.0, 2017.

[96] T. S. Rappaport, Y. Xing, G. R. MacCartney, A. F. Molisch, E. Mellios, and J. Zhang, "Overview of millimeter wave communications for fifth-generation (5G) wireless networks–with a focus on propagation models," *IEEE Trans. Antennas Propag.*, vol. 65, no. 12, pp. 6213–6230, Dec. 2017.

[97] G. R. MacCartney and T. S. Rappaport, "Study on 3GPP rural macrocell path loss models for millimeter wave wireless communications," in *Proc. IEEE Int. Conf. Commun. (ICC)*, no. 1, May 2017, pp. 1–7.

[98] *Study on Channel Model for Frequencies From 0.5 to 100 GHz*, 3GPP TR 38.901, 3rd Generation Partnership Project V14.1.1, 2017.

[99] 5GCM, "White paper on 5G channel model for bands up to 100 GHz," Tech. Rep., 2016. [Online]. Available: http://www.5gworkshops.com/5GCM.html

[100] J. B. Andersen, T. S. Rappaport, and S. Yoshida, "Propagation measurements and models for wireless communications channels," *IEEE Commun. Mag.*, vol. 33, no. 1, pp. 42–49, 1995.

[101] T. S. Rappaport, G. R. MacCartney, M. K. Samimi, and S. Sun, "Wideband millimeter-wave propagation measurements and channel models for future wireless communication system design," *IEEE Trans. Commun.*, vol. 63, no. 9, pp. 3029–3056, Sep. 2015.

[102] S. Sun, T. A. Thomas, T. S. Rappaport, H. Nguyen, I. Z. Kovacs, and I. Rodriguez, "Path loss, shadow fading, and line-of-sight probability models for 5G urban macro-cellular scenarios," in *Proc. IEEE Globecom Workshops (GC Wkshps)*, Dec. 2015, pp. 1–7.

[103] G. R. Maccartney, T. S. Rappaport, S. Sun, and S. Deng, "Indoor office wideband millimeter-wave propagation measurements and channel models at 28 and 73 GHz for ultra-dense 5G wireless networks," *IEEE Access*, vol. 3, pp. 2388–2424, 2015.

[104] S. Piersanti, L. A. Annoni, and D. Cassioli, "Millimeter waves channel measurements and path loss models," in *Proc. IEEE Int. Conf. Commun. (ICC)*, Jun. 2012, pp. 4552–4556.

[105] G. R. MacCartney, J. Zhang, S. Nie, and T. S. Rappaport, "Path loss models for 5G millimeter wave propagation channels in urban microcells," in *Proc. IEEE Global Commun. Conf. (GLOBECOM)*, Dec. 2013, pp. 3948–3953.

[106] *METIS Channel Models*, Standard ICT-317669-METIS/D1.4 ver 3, METIS, 2015.

[107] I. Carton, W. Fan, P. Kyosti, and G. F. Pedersen, "Validation of 5G METIS map-based channel model at mmwave bands in indoor scenarios," in *Proc. 10th Eur. Conf. Antennas Propag. (EuCAP)*, Apr. 2016, pp. 1–5.

[108] *Guidelines for Evaluation of Radio Interface Technologies for IMT-Advanced*, document ITU-R M.2135-1, ITU-R, 2009.

[109] J. Zhang, W. Dong, X. Gao, P. Zhang, and Y. Wu, "Cluster identification and properties of outdoor wideband MIMO channel," in *Proc. IEEE 66th Veh. Technol. Conf.*, Sep. 2007, pp. 829–833.

[110] Y. Lu, J. Zhang, X. Gao, P. Zhang, and Y. Wu, "Outdoor-indoor propagation characteristics of peer-to-peer system at 5.25 GHz," in *Proc. IEEE 66th Veh. Technol. Conf.*, Sep. 2007, pp. 869–873.

[111] X. Gao, J. Zhang, G. Liu, D. Xu, P. Zhang, Y. Lu, and W. Dong, "Large-scale characteristics of 5.25 GHz based on wideband MIMO channel measurements," *IEEE Antennas Wireless Propag. Lett.*, vol. 6, pp. 263–266, Dec. 2007.

[112] D. Xu, J. Zhang, X. Gao, P. Zhang, and Y. Wu, "Indoor office propagation measurements and path loss models at 5.25 GHz," in *Proc. IEEE 66th Veh. Technol. Conf.*, Sep. 2007, pp. 844–848.

[113] J. Zhang, X. Gao, P. Zhang, and X. Yin, "Propagation characteristics of wideband MIMO channel in hotspot areas at 5.25 GHZ," in *Proc. IEEE 18th Int. Symp. Pers., Indoor Mobile Radio Commun.*, 2007, pp. 1–5.

[114] *Measurement Results and Final mmMAGIC Channel Models*, document H2020-ICT-671650-mmMAGIC/D2.2, mmMAGIC, 2015.

[115] *Channel Modeling and Characterization*, document FP&-ICT 368721/D5.1, MiWEBA, 2014, pp. 1–28.

[116] I. A. Hemadeh, K. Satyanarayana, M. El-Hajjar, and L. Hanzo, "Millimeter-wave communications: Physical channel models, design considerations, antenna constructions, and link-budget," *IEEE Commun. Surveys Tuts.*, vol. 20, no. 2, pp. 870–913, 2nd Quart., 2018.

[117] *Final Report on Link Level and System Level Channel Models*, document D5.4 v.1.4, Winner, 2005.

[118] *Winner II Channel Models*, document IST-4-027756 Winner II, D1.1.2 V1.2. 2009.

[119] *Final Channel Models*, document D5.3 v1. CP5-026 Winner, 2010.

[120] P. F. M. Smulders and L. M. Correia, "Characterisation of propagation in 60 GHz radio channels," *Electron. Commun. Eng. J.*, vol. 9, no. 2, pp. 73–80, Apr. 1997.

[121] S. Sun, T. S. Rappaport, T. A. Thomas, A. Ghosh, H. C. Nguyen, I. Z. Kovacs, I. Rodriguez, O. Koymen, and A. Partyka, "Investigation of prediction accuracy, sensitivity, and parameter stability of large-scale propagation path loss models for 5G wireless communications," *IEEE Trans. Veh. Technol.*, vol. 65, no. 5, pp. 2843–2860, May 2016.

[122] S. Sun, T. S. Rappaport, S. Rangan, T. A. Thomas, A. Ghosh, I. Z. Kovacs, I. Rodriguez, O. Koymen, A. Partyka, and J. Jarvelainen, "Propagation path loss models for 5G urban Micro- and macro-cellular scenarios," in *Proc. IEEE 83rd Veh. Technol. Conf. (VTC Spring)*, May 2016, pp. 1–6.

[123] T. A. Thomas, M. Rybakowski, S. Sun, T. S. Rappaport, H. Nguyen, I. Z. Kovacs, and I. Rodriguez, "A prediction study of path loss models from 2–73.5 GHz in an urban-macro environment," in *Proc. IEEE 83rd Veh. Technol. Conf. (VTC Spring)*, May 2016, pp. 1–5.

[124] G. R. MacCartney and T. S. Rappaport, "Rural macrocell path loss models for millimeter wave wireless communications," *IEEE J. Sel. Areas Commun.*, vol. 35, no. 7, pp. 1663–1677, Jul. 2017.

[125] A. M. Al-Samman, T. Abd. Rahman, T. Al-Hadhrami, A. Daho, M. N. Hindia, M. H. Azmi, K. Dimyati, and M. Alazab, "Comparative study of indoor propagation model below and above 6 GHz for 5G wireless networks," *Electronics*, vol. 8, no. 1, p. 44, Jan. 2019.

[126] I. D. S. Batalha, A. V. R. Lopes, J. P. L. Araujo, B. L. S. Castro, F. J. B. Barros, G. P. D. S. Cavalcante, and E. G. Pelaes, "Indoor corridor and office propagation measurements and channel models at 8, 9, 10 and 11 GHz," *IEEE Access*, vol. 7, pp. 55005–55021, 2019.

[127] S. Sun, G. R. MacCartney, and T. S. Rappaport, "A novel millimeter-wave channel simulator and applications for 5G wireless communications," in *Proc. IEEE Int. Conf. Commun. (ICC)*, May 2017, pp. 1–7.

[128] T. S. Rappaport, S. Sun, R. Mayzus, H. Zhao, Y. Azar, K. Wang, G. N. Wong, J. K. Schulz, M. Samimi, and F. Gutierrez, "Millimeter wave mobile communications for 5G cellular: It will work!" *IEEE Access*, vol. 1, pp. 335–349, 2013.

[129] M. K. Samimi and T. S. Rappaport, "3-D millimeter-wave statistical channel model for 5G wireless system design," *IEEE Trans. Microw. Theory Techn.*, vol. 64, no. 7, pp. 2207–2225, Jul. 2016.

[130] S. Sun, G. R. MacCartney, Jr., M. K. Samimi, and T. S. Rappaport, "Synthesizing omnidirectional antenna patterns, received power and path loss from directional antennas for 5G millimeter-wave communications," in *Proc. IEEE Global Commun. Conf. (GLOBECOM)*, Dec. 2015, pp. 1–7.

[131] G. R. MacCartney, Jr., *et al.*, "Millimeter wave wireless communications: New results for rural connectivity," in *Proc. 5th Workshop Things Cellular, Oper. Appl. Challenges, Conjunct. (MobiCom)*, New York, NY, USA, Oct. 2016, pp. 31–36.

[132] H. J. Liebe, G. A. Hufford, and M. G. Cotton, "Propagation modeling of moist air and suspended water/ice particles at frequencies below 1000 GHz," in *Proc. AGARD 52nd Specialists Meeting Electromagn. Wave Propag. Panel*, Palma, Spain, vol. 542, 1993, pp. 3-1–3-10.

[133] A. G. Longley and P. L. Rice, "Prediction of tropospheric radio transmission loss over irregular terrain; A computer method-1968," ESSA, Boulder, CO, USA, Tech Rep. ERL 79-ITS 67, 1968.

[134] P. L. Rice, A. G. Longley, K. A. Norton, and A. P. Barsis, "Transmission loss predictions for tropospheric communication circuits," U.S. Nat. Bureau Standards, Boulder, CO, USA, Tech. Note 101, 1965, vol. 1.

[135] O. Fratu, A. Martian, R. Craciunescu, A. Vulpe, S. Halunga, Z. Zaharis, P. Lazaridis, and S. Kasampalis, "Comparative study of radio mobile and ICS telecom propagation prediction models for DVB-T," in *Proc. IEEE Int. Symp. Broadband Multimedia Syst. Broadcast.*, Jun. 2015, pp. 1–6.

[136] K. Chamberlin and R. Luebbers, "An evaluation of Longley-Rice and GTD propagation models," *IEEE Trans. Antennas Propag.*, vol. 30, no. 6, pp. 1093–1098, Nov. 1982.

[137] P. K. Sharma and R. Singh, "Comparative analysis of propagation path loss models with field measured data," *Int. J. Eng. Sci. Technol.*, vol. 2, no. 6, pp. 2008–2013, 2010.

[138] J. O. Eichie, O. D. Oyedum, M. O. Ajewole, and A. M. Aibinu, "Comparative analysis of basic models and artificial neural network based model for path loss prediction," *Prog. Electromagn. Res. M*, vol. 61, pp. 133–146, Jun. 2017.

[139] L. M. Correia, "A view of the COST 231-Bertoni-Ikegami model," in *Proc. 3rd Eur. Conf. Antennas Propag.*, 2009, pp. 1681–1685.

[140] G. Giusfredi, *Physical Optics: Concepts, Optical Elements, and Techniques*, 1st ed. Milan, Italy: Springer, 2019.

[141] Z. Yun and M. F. Iskander, "Ray tracing for radio propagation modeling: Principles and applications," *IEEE Access*, vol. 3, pp. 1089–1100, 2015.

[142] W. Backman, "Signal level interpolation for coverage area prediction," in *Proc. IEEE 60th Veh. Technol. Conf.*, Sep. 2004, vol. 60, no. 1, pp. 67–71.

[143] G. E. Athanasiadou, A. R. Nix, and J. P. McGeehan, "A microcellular ray-tracing propagation model and evaluation of its narrow-band and wide-band predictions," *IEEE J. Sel. Areas Commun.*, vol. 18, no. 3, pp. 322–335, Mar. 2000.

[144] G. E. Athanasiadou and A. R. Nix, "A novel 3D indoor ray-tracing propagation model: The path generator andevaluation of narrowband and wideband predictions," *IEEE Trans. Veh. Technol.*, vol. 49, no. 4, pp. 1152–1168, Jul. 2000.

[145] G. E. Athanasiadou, E. K. Tameh, and A. R. Nix, "Channel impulse three-dimensional rural-urban simulator (CITRUS): An integrated micro-macro ray-based propagation model which employs raster and vector building databases simultaneously," in *Proc. IEEE PIMRC*, Japan, Sep. 1999, pp. 1072–1076.

[146] G. Liang and H. L. Bertoni, "A new approach to 3-D ray tracing for propagation prediction in cities," *IEEE Trans. Antennas Propag.*, vol. 46, no. 6, pp. 853–863, Jun. 1998.

[147] G. Liang and H. L. Bertoni, "A new approach to 3D ray tracing for site specific propagation modeling," in *Proc. IEEE 47th Veh. Technol. Conf. Technol. Motion*, May 1995, pp. 1113–1117.

[148] S. Y. Seidel and T. S. Rappaport, "Site-specific propagation prediction for wireless in-building personal communication system design," *IEEE Trans. Veh. Technol.*, vol. 43, no. 4, pp. 879–891, 1994.

[149] K. Rizk, J.-F. Wagen, and F. Gardiol, "Two-dimensional ray-tracing modeling for propagation prediction in microcellular environments," *IEEE Trans. Veh. Technol.*, vol. 46, no. 2, pp. 508–518, May 1997.

[150] J. W. McKown and R. L. Hamilton, "Ray tracing as a design tool for radio networks," *IEEE Netw.*, vol. 5, no. 6, pp. 27–30, Nov. 1991.

[151] F. Villanese, W. G. Scanlon, N. E. Evans, and E. Gambi, "Hybrid image/ray-shooting UHF radio propagation predictor for populated indoor environments," *Electron. Lett.*, vol. 35, no. 21, pp. 1804–1805, Oct. 1999.

[152] G. E. Athanasiadou and I. J. Wassell, "Comparisons of ray tracing predictions and field trial results for broadband fixed wireless access scenarios," *WSEAS Trans. Commun.*, vol. 4, no. 8, pp. 717–721, 2005.

[153] A. Goldsmith, *Wireless Communications*. Cambridge, U.K.: Cambridge Univ. Press, 2005.

[154] K. Yee, "Numerical solution of initial boundary value problems involving Maxwell's equations in isotropic media," *IEEE Trans. Antennas Propag.*, vol. 14, no. 3, pp. 302–307, May 1966.

[155] A. Valcarce, G. De La Roche, and J. Zhang, "A GPU approach to FDTD for radio coverage prediction," in *Proc. 11th IEEE Singapore Int. Conf. Commun. Syst.*, Nov. 2008, pp. 1585–1590.

[156] A. Valcarce, G. De La Roche, Á. Jüttner, D. López-Pérez, and J. Zhang, "Applying FDTD to the coverage prediction of wiMAX femtocells," *Eurasip J. Wireless Commun. Netw.*, vol. 2009, p. 13, Mar. 2009.

[157] J. W. Schuster and R. J. Luebbers, "Comparison of GTD and FDTD predictions for UHF radio wave propagation in a simple outdoor urban environment," in *IEEE Antennas Propag. Soc. Int. Symp. Dig.*, vol. 3, Jul. 1997, pp. 2022–2025.

[158] G. D. Kondylis, F. De Flaviis, G. J. Pottie, and Y. Rahmat-Samii, "Indoor channel characterization for wireless communications using reduced finite difference time domain (R-FDTD)," in *Proc. Gateway 21st Century Commun. Village. VTC-Fall IEEE VTS 50th Veh. Technol. Conf.*, vol. 3, 1999, pp. 1402–1406.

[159] A. Lauer, I. Wolff, A. Bahr, J. Pamp, J. Kunisch, and I. Wolff, "Multimode FDTD simulations of indoor propagation including antenna properties," in *Proc. IEEE 45th Veh. Technol. Conf. Countdown Wireless 21st Century*, vol. 1, Jul. 1995, pp. 454–458.

[160] Y. Wang, S. Safavi-Naeini, and S. K. Chaudhuri, "A hybrid technique based on combining ray tracing and FDTD methods for site-specific modeling of indoor radio wave propagation," *IEEE Trans. Antennas Propag.*, vol. 48, no. 5, pp. 743–754, May 2000.

[161] D. K. Price, J. R. Humphrey, and E. J. Kelmelis, "GPU-based accelerated 2D and 3D FDTD solvers," *Proc. SPIE*, vol. 6468, Mar. 2007, Art. no. 646806.

[162] J. R. Humphrey, D. K. Price, J. P. Durbano, E. J. Kelmelis, and R. D. Martin, "High performance 2D and 3D FDTD solvers on GPUs," in *Proc. 10th WSEAS Int. Conf. Appl. Math.*, 2006, pp. 547–550.

[163] R. N. Schneider, M. M. Okoniewski, and L. E. Turner, "A software-coupled 2D FDTD hardware accelerator [electromagnetic simulation]," in *Proc. IEEE Antennas Propag. Soc. Symp.*, vol. 2, Jun. 2004, pp. 1692–1695.

[164] D. Deligiorgi, K. Philippopoulos, and G. Kouroupetroglou, "Artificial neural network based methodologies for the spatial and temporal estimation of air temperature," in *Proc. Int. Conf. Pattern Recognit. Appl. Methods*, 2013, pp. 669–678.

[165] A. Nesković, N. Nesković, and D. Paunović, "Indoor electric field level prediction model based on the artificial neural networks," *IEEE Commun. Lett.*, vol. 4, no. 6, pp. 190–192, Jun. 2000.

[166] M. Hassoun, *Fundamentals of Artificial Neural Networks*. Cambridge, MA, USA: MIT Press, 1995.

[167] K. E. Stocker and F. M. Landstorfer, "Empirical prediction of radiowave propagation by neural network simulator," *Electron. Lett.*, vol. 28, no. 12, pp. 1177–1178, Jun. 1992.

[168] I. Popescu, D. Nikitopoulos, P. Constantinou, and I. Nafornita, "ANN prediction models for outdoor environment," in *Proc. IEEE 17th Int. Symp. Pers., Indoor Mobile Radio Commun.*, Sep. 2006, pp. 1–5.

[169] Z. Stankovic, B. Milovanvic, M. Veljkovic, and A. Dordevic, "The hybrid-neural empirical model for the electromagnetic field level prediction in urban environments," in *Proc. 7th Seminar Neural Netw. Appl. Electr. Eng. (NEUREL)*, 2004, pp. 189–192.

[170] E. Ostlin, H. Zepernick, and H. Suzuki, "Macrocell path-loss prediction using artificial neural networks," *IEEE Trans. Veh. Technol.*, vol. 59, no. 6, pp. 2735–2747, Jul. 2010.

[171] Y. Zhang, J. Wen, G. Yang, Z. He, and J. Wang, "Path loss prediction based on machine learning: Principle, method, and data expansion," *Appl. Sci.*, vol. 9, no. 9, p. 1908, May 2019.

[172] Y. Wu, M. Lin, and I. Wassell, "Path loss estimation in 3D environments using a modified 2D finite-difference time- domain technique," in *Proc. IET 7th Int. Conf. Comput. Electromagn. (CEM)*, no. 4, 2008, pp. 98–99.

[173] W. C. Y. Lee, *Mobile Communications Design Fundamentals*. Hoboken, NJ, USA: Wiley, 1993.

[174] M. A. ElMossallamy, H. Zhang, L. Song, K. G. Seddik, Z. Han, and G. Y. Li, "Reconfigurable intelligent surfaces for wireless communications: Principles, challenges, and opportunities," *IEEE Trans. Cogn. Commun. Netw.*, early access, May 2020, doi: 10.1109/TCCN.2020.2992604.

[175] S. Hu, F. Rusek, and O. Edfors, "Beyond massive MIMO: The potential of data transmission with large intelligent surfaces," *IEEE Trans. Signal Process.*, vol. 66, no. 10, pp. 2746–2758, May 2018.
[176] H. Guo, Y.-C. Liang, J. Chen, and E. G. Larsson, "Weighted sum-rate maximization for intelligent reflecting surface enhanced wireless networks," in *Proc. IEEE Global Commun. Conf. (GLOBECOM)*, Dec. 2019, pp. 1–6.
[177] C. Liaskos, S. Nie, A. Tsioliaridou, A. Pitsillides, S. Ioannidis, and I. Akyildiz, "A new wireless communication paradigm through software-controlled metasurfaces," *IEEE Commun. Mag.*, vol. 56, no. 9, pp. 162–169, Sep. 2018.

CASPAR K. LEBEKWE (Member, IEEE) received the M.Eng. degree in electronics and communications engineering from the University of Bath in 2008, and the Ph.D. degree in electrical and electronics engineering from the University of Bath, sponsored by the General Lighthouse Authorities. His Ph.D. project was focused on eLoran service volume coverage prediction. He is currently a Lecturer with the Botswana International University of Science and Technology, where he teaches optical communications, antennas and propagation, discrete mathematics, telemetry, and remote control as well as electromagnetic field theory.

OLAONIPEKUN OLUWAFEMI ERUNKULU (Member, IEEE) received the B.Eng. degree in electrical and computer engineering and the M.Eng. degree in communications engineering from the Federal University of Technology, Minna, Nigeria, in 2004 and 2016, respectively. He is currently pursuing the Ph.D. degree with Electrical, Computer and Telecommunications Department, Botswana International University of Science and Technology, Palapye, Botswana. He is a Lecturer with the Department of Computer Engineering, Federal University of Technology.

ADAMU MURTALA ZUNGERU (Senior Member, IEEE) received the B.Eng. degree from the Federal University of Technology, Minna, Nigeria, the M.Sc. degree from Ahmadu Bello University, Zaria, Nigeria, and the Ph.D. degree from Nottingham University, U.K. He was a Research Fellow with the Massachusetts Institute of Technology (MIT), USA, where he also obtained a Postgraduate Teaching Certificate, in 2014. He is currently serving as a Professor and the Head of the Department of Electrical, Computer, and Telecommunications Engineering, Botswana International University of Science and Technology (BIUST). Before joining BIUST, in 2015, he was a Senior Lecturer and the Head of the Electrical and Electronics Engineering Department, Federal University Oye-Ekiti, Nigeria. He is a Registered Engineer with the Council for The Regulation of Engineering in Nigeria (COREN) and the Association for Computing Machinery (ACM), USA. He is the Inventor of a Termite-hill routing algorithm for wireless sensor networks. He has two of his patent applications registered with the World Intellectual Property Organization (WIPO). He has also authored four academic books and over 60 international research articles in reputable journals, including the IEEE Systems Journal, the IEEE Internet of Things Journal, IEEE Access, JNCA (Elsevier), and others, with over 900 citations and H-index of 14. He has also served as an International Reviewer of the IEEE Transactions on Industrial Informatics, the IEEE Sensors, IEEE Access, the IEEE Transactions on Mobile Computing, the IEEE Transactions on Sustainable Computing, JNCA (Elsevier), and numerous others. He has also served as the Chairman of the IEEE Botswana Sub-Section (2019–2020), and currently serving as the IEEE Region 8 Vitality and Development Subcommittee Member.

JOSEPH M. CHUMA (Member, IEEE) received the Ph.D. degree in electronic systems engineering from the University of Essex, in 2001. He was with the University of Botswana as an Associate Professor and the Dean of the Faculty of Engineering and Technology, and he is currently a Full Professor and serving as the Acting Deputy Vice-Chancellor for Research, Development, and Innovation. He is also the Substantive Dean of the Faculty of Engineering and Technology, Botswana International University of Science and Technology. He has over 24 years of experience in teaching and research, consultancy, and human resources development in telecommunication, computer, and electrical and electronics engineering, including CISCO computer networking. He has authored or coauthored three books, three book chapters, and many refereed published scholarly/scientific journal articles in the subject of telecommunications engineering. He holds three patents. He is a member of several professional bodies, among which includes the IEEE, USA; IET, U.K.; and BIE, Botswana. He is a Professional Engineer registered with the Botswana Engineers Registration Board.

● ● ●